Action and Semantic Tool Knowledge – effective connectivity in the underlying neural networks

Nina N. Kleineberg[1,2], Anna Dovern[1], Ellen Binder[2], Christian Grefkes[1,2], Simon B. Eickhoff[3,4], Gereon R. Fink[1,2], Peter H. Weiss[1,2,#]

[1] *Cognitive Neuroscience, Institute of Neuroscience and Medicine (INM-3), Research Center Jülich, Germany*

[2] *Department of Neurology, University Hospital Cologne, Germany*

[3] *Institute for Systems Neuroscience, Heinrich Heine University Düsseldorf, Germany*

[4] *Brain and Behaviour, Institute of Neuroscience and Medicine (INM-7), Research Center Jülich, Germany*

[#]**Corresponding author:**

Dr. Peter H. Weiss
Cognitive Neuroscience
Institute of Neuroscience and Medicine (INM-3)
Forschungszentrum Jülich
Leo-Brandt-Str. 5
52425 Jülich, Germany
Email: P.H.Weiss@fz-juelich.de
Tel.:   02461-61-2073
Fax: 02461-61-1518

Short title: Effective Connectivity in Tool Knowledge

Keywords: tool knowledge, visuo-motor streams, action representations, parietal lobe, lateral occipito-temporal cortex, dynamic causal modelling (DCM), effective connectivity, apraxia

Abstract

Objectives. Evidence from neuropsychological and imaging studies indicate that action and semantic knowledge about tools draw upon distinct neural substrates, but little is known about the underlying interregional effective connectivity.

Experimental design. With fMRI and dynamic causal modeling (DCM) we investigated effective connectivity in the left-hemisphere (LH) while subjects performed (i) a function knowledge and (ii) a value knowledge task, both addressing semantic tool knowledge, and (iii) a manipulation (action) knowledge task.

Principal observations. Overall, the results indicate crosstalk between action nodes and semantic nodes. Interestingly, effective connectivity was weakened between semantic nodes and action nodes during the manipulation task. Furthermore, pronounced modulations of effective connectivity within the fronto-parietal action system of the LH (comprising lateral occipito-temporal cortex, intraparietal sulcus, supramarginal gyrus, inferior frontal gyrus) were observed in a bidirectional manner during the processing of action knowledge. In contrast, the function and value knowledge tasks resulted in a significant strengthening of the effective connectivity between visual cortex and fusiform gyrus. Importantly, this modulation was present in both semantic tasks, indicating that processing different aspects of semantic knowledge about tools evokes similar effective connectivity patterns.

Conclusions. Data revealed that interregional effective connectivity during the processing of tool knowledge occurred in a bidirectional manner with a weakening of connectivity between areas engaged in action and semantic knowledge about tools during the processing of action knowledge. Moreover, different semantic tool knowledge tasks elicited similar effective connectivity patterns.

Introduction

Differential impairments of tool knowledge due to neurological disease indicate that knowledge about action and semantic aspects of tools draw upon distinct neural networks. Impaired manipulation knowledge (action knowledge), i.e., knowing how to handle / manipulate a tool, is a key deficit in patients suffering from apraxia (Buxbaum, et al., 2000), who often exhibit parietal lesions (Martin, et al., 2016b; Niessen, et al., 2014). The role of the left inferior parietal cortex (IPL) and left intraparietal sulcus (IPS) in action representation is corroborated by many imaging studies that contrast tasks requiring manipulation knowledge about tools with function knowledge (i.e., knowing what a tool is used for, semantic knowledge) (Boronat, et al., 2005; Canessa, et al., 2008; Chen, et al., 2017b; Kellenbach, et al., 2003) and by non-invasive brain stimulation studies (Andres, et al., 2013; Evans, et al., 2016; Ishibashi, et al., 2011).

In contrast, patients with semantic dementia (SD) or other causes of temporal lobe damage often show deficits concerning the semantic knowledge about tools, e.g., impaired identification of tools and/ or impaired function knowledge about tools, while praxis skills of the same tool can remain unaffected (Baumard, et al., 2017; Buxbaum, et al., 1997; Lauro-Grotto, et al., 1997; Magnie, et al., 1999; Martin, et al., 2016a; Negri, et al., 2007; Sirigu, et al., 1991). Imaging studies contrasting function knowledge with manipulation knowledge revealed activity in the lateral anterior infero-temporal lobe (ATL) (Canessa, et al., 2008; Chen, et al., 2016) and the medial fusiform gyrus (FFG) (Chen, et al., 2017b). Consistent with these imaging findings, non-invasive brain stimulation over the ATL affected function judgment tasks (Andres, et al., 2013; Ishibashi, et al., 2011; Ishibashi, et al., 2017).

This double dissociation regarding differential tool-related deficits in patients with apraxia (and lesions of the parietal cortex) versus those of SD patients (with lesions of the temporal cortex) are consistent with the hypothesis of two segregated functional visuo-motor streams: a dorsal stream and a ventral stream, that were originally presumed as processing pathways for vision-for-action ('where') and vision-for-perception ('what'), respectively (Goodale and Milner, 1992; Ungerleider and Mishkin, 1982). In this framework, the ventral stream mediates semantic aspects of tools and the dorsal stream mediates online control of tool-associated actions.

A recent extension of the two-stream model posits a further subdivision of the dorsal stream into a dorso-dorsal stream and a ventro-dorsal stream (Binkofski and Buxbaum, 2013). Here, the dorso-dorsal stream is thought to process structural object properties for prehensile actions ('grasp system') and supports online-motor control, while the ventro-dorsal stream represents the 'use system' for skilled actions with (familiar) objects and supports long-term tool action representations (Binkofski and Buxbaum, 2013; Buxbaum and Kalenine, 2010; Hoeren, et al., 2014; Rizzolatti and Matelli, 2003). In this context, optic ataxia is a typical disorder caused by lesions to the dorso-dorsal stream resulting in deficient reaching, whereas limb apraxia is commonly associated with ventro-dorsal stream lesions, in which online motor control remains intact (Binkofski and Buxbaum, 2013).

Anatomically, the origin of the visuo-motor streams is the primary visual area (V1). From here, the ventral stream projects along the occipital and temporal cortices, including the FFG and the ATL (Mahon, et al., 2007). The dorsal stream projects from V1 towards the parietal lobe, in which the superior parietal lobe (SPL) serves as a key player in the dorso-dorsal stream, while the inferior parietal lobe (IPL) and parts of the anterior intraparietal sulcus (aIPS) are

important nodes within the ventro-dorsal stream (Binkofski and Buxbaum, 2013; Grefkes and Fink, 2005; Sakreida, et al., 2016).

Nevertheless, the concept of segregated action and semantic representations falls short in explaining various complex findings. For instance, the well-known patient DF, suffering from visual agnosia due to ventral lesions, fails to grasp objects in a functionally appropriate manner despite an intact parietal and frontal lobe (Carey, et al., 1996; Milner, 1997). Likewise, in SD the degraded conceptual semantic information about tools is sometimes associated with impaired tool use/ action knowledge (Hodges, et al., 2000; Hodges, et al., 1999). A 4-year longitudinal study showed that such tool-use deficits in SD developed with the decline of conceptual knowledge about tools and indicate the relevance of semantic knowledge for praxis skills (Coccia, et al., 2004). In the same vein, apraxic patients may also show deficits in function knowledge about tools as reflected, e.g., in content errors during actual tool use (De Renzi and Lucchelli, 1988; Martin, et al., 2016a; Ochipa, et al., 1989). These findings suggest that besides the integrity of the visuo-motor streams, also an adequate information exchange between the streams may be requisite for the proper processing of tool knowledge and tool use.

However, to date only few studies addressed the issue of (functional or effective) connectivity within and between the nodes of the visuo-motor streams. An interesting set of imaging studies found that in the context of tool action representations, the IPL gets input via ventral areas (Almeida, et al., 2013; Garcea, et al., 2016; Kristensen, et al., 2016; Mahon, et al., 2013). These findings suggest that an object's identification and function is first decoded by ventral regions, and then this information is communicated to the IPL, where it is combined with information processed by dorsal regions (e.g., position, orientation) in order to perform adequate tool manipulation (Kristensen, et al., 2016).

Here, we aimed at extending those previous findings by investigating the effective connectivity during the processing of action and semantic knowledge about tools with fMRI and dynamic causal modeling (DCM).

In the imaging experiment, we used a manipulation (action) knowledge task (i.e., which of two hand postures is appropriate for using the target tool?) and two semantic knowledge tasks: a function knowledge task (i.e., which of two recipient objects is typically used together with the target tool?), and a value estimation task (i.e., what is the approximate monetary value of the target tool?).

Due to the fact that (i) semantic knowledge about tools comprises various aspects in addition to function knowledge and (ii) that many studies found action knowledge to be contingent on function knowledge, the value estimation task was chosen as an additional semantic task, with clearly no relevance for manipulation. Separate exploration of the effective connectivity patterns during these two semantic tasks (processing of function and value knowledge) was of interest to reveal whether processing of semantic knowledge is generalizable across the different semantic aspects of tool knowledge.

The resulting fMRI data were first evaluated by a conventional general linear model (GLM). Based on these GLM results, we then focused on the context-dependent effective connectivity (Friston, et al., 2003).

Materials and Methods

Participants

Twenty healthy participants gave written informed consent to participate in the study. Due to technical problems two subjects had to be excluded from the final analyses. Therefore, data from 18 subjects were analyzed (10 female; mean age 25.3 years, range 18 to 35 years). All participants had normal or corrected to normal vision and were right-handed (Oldfield, 1971). The study was conducted in accordance with the Declaration of Helsinki and was approved by the local ethics committee.

Stimuli and Task

The study featured three experimental conditions. For each of these (manipulation knowledge condition (M), function knowledge condition (F), and monetary value knowledge condition (V)), 40 stimuli per task were created based on an identical set of uni-manually manipulable tools used in all three conditions (see **Suppl. Table SIV**). During the functional magnetic resonance imaging (fMRI) experiment, visual stimuli were presented on a 30''shielded TFT (thin film transistor) monitor mounted 245 cm behind the scanner. Stimuli were viewed via a mirror installed on top of the head coil. The size of the stimuli displayed on the TFT screen corresponded to a visual angle of 13.8° x 8.2°. For stimulus presentation and response monitoring, the Presentation Software package (Neurobehavioral Systems Inc., Berkeley, CA/USA) was used.

In the 'manipulation' condition (M), stimuli consisted of a target tool and photographs of two different hand postures. The target tool, surrounded by a black frame, was presented centrally in the lower part of the stimulus display. The pictures of the two hand postures were presented simultaneously in the upper right and left corners of the stimulus display, one being

suitable for manipulating the tool and the other one not. In the 'function' condition (F), stimuli were composed of a target tool and pictures of two objects, with one of these two objects functionally related to the target tool and the other not. Finally, stimuli in the 'monetary value' condition (V) contained pictures of the same target tools in combination with two pictures of coins (1 or 2 Euro coin) or banknotes (5, 10, 20, or 50 Euro note). One of the depicted amounts of money approximated the true value of the target tool whereas the other was clearly too high or low (see **Figure 1** for experimental stimuli in the three tasks and **Suppl. Table SIV** for displayed items, coins and banknotes).

Participants were asked to examine the stimuli and to judge whether the hand posture (M), the object (F), or the monetary value (V) presented on the left or right side fitted the target tool better. Participants indicated their choice by pressing one of two buttons with the index or the middle finger of the left hand. The left hand was used to minimize any confounding effects of motor execution on left-hemispheric activations. The chosen picture corresponded spatially to the left- / right-sided response key (i.e., left-sided picture / middle finger, right-sided picture / index finger).

Procedure and Design

Before entering the scanner, participants were familiarized with the tasks. Practice trials did not re-appear in the actual fMRI experiment to avoid learning effects. Participants were asked to respond both as accurately and as fast as possible.

The study employed a blocked within-subject design alternating experimental blocks (duration 28 s) with baseline (duration 22 s) to maximize design efficiency (Mechelli, et al., 2003). During the low-level baseline period, subjects were shown a white screen with a black frame (surrounding the target tool in the experimental conditions) only. After 20 s the color of the

frame changed to red indicating the start of the next task-block in 2 s. Five blocks, each containing eight trials, were presented per experimental condition (M, F, and V), yielding a total of 15 experimental blocks. Stimulus duration was fixed (3500 ms) with no inter-stimulus interval. The order of the stimuli was randomized, while the order of blocks was pseudo-randomized. During the fMRI-experiment reaction times and accuracy were recorded.

fMRI data acquisition and preprocessing

A 3-Tesla MRI System (Trio, Siemens, Erlangen, Germany) was used to obtain T2*-weighted gradient echo-planar images (EPI) with BOLD contrast (matrix size: 64 x 64; voxel-size: $3.1 \times 3.1 \times 3.0$ mm³; field of view: 200 mm; repetition time: 2200 ms; echo time: 30 ms; flip angle: 90°). Thirty-six transversal slices of 3 mm thickness were acquired sequentially with a 0.3 mm interslice gap (whole-brain coverage). A total of 362 functional volumes were collected for each subject in a single functional run. FMRI data were analyzed using the Statistical Parametric Mapping software package (SPM8, Wellcome Department of Imaging Neuroscience, London; http://www.fil.ion.ucl.ac.uk/spm). The effective connectivity analysis was conducted using the latest DCM code as implemented in SPM12 (version: Oct 20, 2016). The first six EPI volumes were omitted to allow for T1 equilibration effects. In order to correct for inter-scan movements, EPI images were first spatially realigned. Then, the mean EPI image for each participant was computed and spatially normalized to the Montreal Neurological Institute (MNI) template using the "unified segmentation" function in SPM8 (Ashburner and Friston, 2005). Finally, the data were smoothed using a Gaussian kernel of 8 mm full width half maximum (FWHM) to suppress noise.

Data analyses

Data processing

Analyses of the behavioral data were performed using SPSS (IBM SPSS Statistics, Version 21). For the statistical analysis of the BOLD data, three regressors of interest containing the onset and duration of the three experimental conditions were defined. The BOLD response was modeled using a canonical hemodynamic response function and its first derivative. Moreover, head movement parameters were included as additional regressors of no interest in the design matrix. Baseline periods were not explicitly modeled.

The three simple contrasts (i.e., the three experimental conditions each compared with the implicit baseline) were specified at the first-level and then transferred to a second-level ANOVA model. At the second level, all six differential contrasts were calculated (M>F, M>V, F>M, V>M, F>V, V>F). As expected, the semantic tool knowledge tasks (F and V) revealed similar behavioral effects and engaged similar brain regions in fMRI, affirmed by a conjunction analysis of the contrasts F>M and V>M (for Results see **Suppl. Table SI and SII)**. Therefore, and in order to identify robust activations of brain regions engaged in action knowledge (here: M) and semantic knowledge (here: F and V) about tools, the following additional differential contrasts were specified: 2*M>(F+V) and vice versa (F+V)>2*M (cf. **Table I**; see Results).

All differential contrasts were thresholded at p<0.05, family wise error (FWE)-corrected for multiple comparison at the voxel level, to adjust for falsely positive voxels (Nichols and Hayasaka, 2003). Note that voxel-wise inference is considered more robust than cluster-size inference, since voxel-wise inference is not affected by the recently discussed problems caused by too liberally defined cluster thresholds (Eklund, et al., 2016; Woo, et al., 2014). In addition, an extent threshold of 100 voxels was applied for the six simple contrasts and 2*M>(F+V) and (F+V)>2*M.

Dynamic causal modelling (DCM)

We used dynamic causal modelling (Friston, et al., 2003) to study the underlying effective connectivity in the neural network engaged in processing different aspects of tool knowledge. DCM is a hypothesis-driven approach to make interferences about neural connectivity in terms of direction and effect size (using the parameter 'rate constant' with the unit Hertz (1/s), while the influence that one region exerts upon another can be positive or negative). Note that obtained connectivity parameters may not necessarily reflect monosynaptic anatomical connections but rather the net effect, for example, transmitted via direct connections, a single relay area or more extensive loops (Stephan, et al., 2009b).

For DCM analyses, the 'model space' must be defined *a priori*, i.e., different plausible network models need to be generated beforehand. Subsequently, the competing models are fed with the underlying data of all subjects in form of subject-specific volumes of interest (VOIs). Finally, based on Bayesian model selection (BMS) the model that best explains the underlying fMRI data is identified as 'winning model'.

The (dynamic) changes in the neural model over time ($\dot{z}$) assumed by DCM are represented in the bilinear state equation $\dot{z} = (A + \sum_j u_j B^j) z + Cu$ (Friston, et al., 2003). The A-matrix represents the task-independent intrinsic (fixed) connectivity, the B-matrix the task-dependent modulations of A, and the C-matrix the direct input to the system.

Regions of interest (ROI)

The selection of regions of interest was based on the results of the GLM analysis. Since the number of regions of interest (ROI) in the computation of a DCM analysis is limited (Daunizeau, et al., 2011; Stephan, et al., 2010), we included only the eight regions in the *left* hemisphere (LH) that had shown significant activation in the differential contrasts 2*M>(F+V) or

(F+V)>2*M, which is clinically plausible, since tool use deficits are most often observed after LH lesions (Martin, et al., 2016a; Martin, et al., 2016b).

Thus, the VOIs for the eight left hemispheric regions were obtained for each participant at the individual level. Given the results of the GLM analysis, the VOIs for the lateral occipito-temporal cortex (LOTC), intraparietal sulcus (IPS), supramarginal gyrus (SMG), and inferior frontal gyrus (IFG) of the LH were based on the contrast 2*M>(F+V), while the reverse contrast (F+V)>2*M was applied to obtain the VOIs for the left fusiform gyrus (FFG), the left angular gyrus (AG), and the medial prefrontal cortex (mPFC) (cf. **Table I**). The coordinates for the early visual region (visual area 1 and 2, V1/2), as common input region, were selected based upon a conjunction analysis of all three conditions (M, F, and V) versus baseline (Friston, et al., 2005; Nichols, et al., 2005).

Mostly the individual local maximum, in some cases a sub-maximum to fit the anatomical constraints of the identified ROI was chosen for time-series extraction (see **Suppl. Table SIII** for the individual MNI coordinates and the respective anatomical localization assessed with the Anatomy Toolbox (Version 2.2c), implemented in SPM12 (Eickhoff, et al., 2005). For a visual depiction of the individual maxima see **Fig. 3**. Computation of the individual Euclidean distances between the MNI coordinates ruled out any potential VOI overlap. The shortest distance between two VOIs was 17 mm (between IPS and AG).

Time series of the VOIs were extracted for supra-threshold voxels as the first eigenvariate within a sphere of 3 mm radius around the individual (sub-)maxima at a threshold of $p<0.001$ (uncorrected) and, if necessary, gradually lowered to $p<0.05$ (uncorrected). In one subject the eight VOIs could not be reliably identified, so data from this subject could not be included into the connectivity analysis.

Generation of models for DCM/ the model space

The different models, grouped into model families (see (Penny, et al., 2010)) were specifically generated to examine two main aspects of the network processing tool knowledge.

Given that action and semantic knowledge about tools are processed by different brain regions/nodes, we first created four different model families (F1 – F4) that varied with respect to putative *interactions* between semantic nodes and action nodes, i.e., structural differences in the A-matrix (see **Suppl. Figure S1a**): model family F1, no interaction; model family F2, interaction within the occipito-temporal lobe (FFG–LOTC); model family F3, interaction within the parietal lobe, (AG–SMG); and model family F4, interactions within both, the occipito-temporal and the parietal lobe (FFG–LOTC, AG–SMG).

Second, different hypotheses about the task-dependent *modulation* of effective connectivity by the three experimental tasks (B-matrices for M, F, V) lead to six models within each model family (see **Suppl. Figure S1b-e)**: three different levels of modulations were assumed; (i) modulatory effects within the occipito-temporal lobe only (V1/2, LOTC, FFG); (ii) modulatory effects throughout the occipito-temporal lobe and parietal lobe (V1/2, LOTC, FFG, IPS, SMG, AG); and (iii) modulatory effects at all (three) levels, i.e., throughout the occipito-temporal lobe, the parietal lobe and the frontal lobe (V1/2, LOTC, FFG, SMG, AG, IFG, mPFC). All these different hypotheses were configured as (a) unidirectional and (b) bidirectional to examine whether the experimental conditions (M, F, and V) modulated the connectivity between involved brain regions/ nodes in only one direction or in a bidirectional manner.

Accordingly, the investigated aspects led to a total of 24 models: four model families (F1 – F4, different interactions between action nodes and semantic nodes) with six models each (six = three (different levels of modulation) times two (unidirectional versus bidirectional)). For an overview of all 24 considered models see **Suppl. Figure S1**.

Note that similar differential *activity* patterns in the GLM (as for the F and V task) do not necessarily imply that the activated regions reveal analogous *connectivity* patterns. Thus, all three tasks (M, F, and V) were implemented as separate B-matrices to explore whether the effective connectivity patterns for processing of semantic aspects about tools could be generalized across different semantic conditions.

After the different models were established and fed with the underlying fMRI data, a random-effects Bayesian model selection (BMS) was applied to identify the 'winning' model family of the 4 families, and the 'winning' single model, i.e., the one with highest evidence in explaining the given data out of all tested model families/ single models. This superiority can be expressed by its exceedance probability (in %) in relation to the tested alternatives (Stephan, et al., 2009a). Hence, the model parameters (A-, B-,and C-matrices) were extracted for each subject, then averaged across subjects and tested for significance by one-sample t-tests ($p < 0.05$, corrected for multiple comparisons by false discovery rate (FDR) (Benjamini and Hochberg, 1995)).

Finally, the total mean variance between prior and posterior parameters (i.e., the mathematical model and the observed data) explained by the winning model was computed with the spm_dcm_fmri_check.m script provided in the SPM helpline by Karl Friston (2012; https://www.jiscmail.ac.uk/cgi-bin/webadmin? A2=spm;bebd494.1203).

Results

Behavioral Data

One-way repeated measures ANOVAs revealed that accuracy was similar across tasks (M: 94.7 %, F: 95.3 %, V: 94.7 %; $F_{(2,34)} < 1$). However, a significant difference with respect to reaction times (RTs) was observed ($F_{(2,34)} = 77.9$, $p < .001$). Post-hoc comparisons revealed that the RTs of the action knowledge task (M) were systematically longer than those of the semantic knowledge tasks (F and V), which did not differ significantly from each other (M [mean ± SD]: 1758 ± 176 ms, F: 1329 ± 172 ms, V: 1398 ± 233 ms; M vs F: $t_{(17)} = 17.1$, $p < .001$; M vs V $t_{(17)} = 8.7$, $p < .001$; F vs V: $t_{(17)} = 1.7$, $p = .117$).

Functional Imaging

GLM analysis

As expected, the simple contrasts of M>F, M>V, F>M, F>V, V>M, and V>F revealed highly similar activation patterns for the two semantic tool knowledge tasks (F and V). The similarity of the activity patterns for F and V was further supported by a conjunction analysis of the contrasts F>M and V>M. These results are reported in the Supplementary Material as the focus of this study was on the effective connectivity analysis, which was based on the GLM results.

For the direct comparison of action knowledge and semantic knowledge about tools, we contrasted in the GLM analysis the M task with the F and V task (i.e., 2*M>(F+V)) yielding significant activation clusters in the LOTC bilaterally, the left IPS, the left SMG, and the left IFG (see **Table I** and **Figure 2,** activations in red). The reverse contrast ((F+V)>2*M) revealed significant activation clusters in the FFG and the AG bilaterally as well as in the mPFC (see **Table I** and **Figure 2**, activations in blue).

DCM results

Family 4 was superior to the other tested hypotheses with an exceedance probability of 73.6 % (see **Table IIa**). As a common feature, all models of family 4 postulated couplings *between* the regions processing action knowledge (action nodes) and semantic knowledge about tools (semantic nodes) within the occipito-temporal lobe (LOTC–FFG) and the parietal lobe (SMG– AG). Out of the 24 tested models the individual model F4M2 belonging to family 4 had the highest evidence for explaining the underlying data with an exceedance probability of 54.4 % (see **Table IIb**). Please note, that in Bayesian Model Selection (BMS), models with more degrees of freedom are penalized to balance the benefit of complexity in fitting the data with the loss of accuracy (Penny, et al., 2004; Stephan, et al., 2009b). With respect to the divergence between prior and posterior parameter distributions, we computed the total mean variance explained. On average across subjects our winning model explained 40.0 % ± SD 11.5 % of the variance (range 19 % to 59 %) indicating a good fit of predicted and observed responses.

Effective connectivity during the processing of tool knowledge

Readout of the winning model F4M2 across subjects revealed the following significant ($p<0.05$, FDR-corrected) mean intrinsic effective connectivity patterns (A-matrix): from more caudal nodes to more rostral nodes positive intrinsic couplings were revealed (action nodes: V1/2→LOTC→IPS, SMG→IFG; and semantic nodes: V1/2→FFG, AG→mPFC), and in the opposite direction negative intrinsic couplings (action nodes: IFG→SMG; and semantic nodes: mPFC→AG, FFG→V1/2) (see **Figure 4a** and **Table III**).

Directed modulatory effects (B-matrix) during the manipulation task further strengthened the above mentioned intrinsic positive couplings (V1/2→LOTC→IPS→SMG→IFG), while – in

opposite direction connectivity was weakened (IFG→SMG→IPS→LOTC) (see **Figure 4b**, action nodes = ROIs on the left; and **Table III**).

The modulatory effects of both semantic tasks (F and V) were not as pronounced, revealing only one significant modulation: from V1/2 to FFG. Interestingly, this (one) modulatory effect was similar in the F and V task (same direction, same effect (positive) and similar effect strength: V: +0.05 Hz, F: +0.76 Hz; see **Figure 4c** and **4d**, semantic nodes = ROIs on the right; and **Table III**), indicating that processing different aspects of semantic knowledge exert similar interregional effective connectivity (see discussion).

Effective connectivity between action nodes and semantic nodes

Overall, the results indicated superiority of models that assumed couplings *between* semantic nodes and action nodes, namely couplings within the occipito-temporal lobe (FFG–LOTC) and within the parietal lobe (AG–SMG). Intrinsic couplings between action nodes and semantic nodes revealed a significant ($p < 0.05$, FDR-corrected), but minor positive connectivity (+0.05 Hz): from SMG to AG (see **Figure 4a**). Interestingly, this connection was strongly weakened by the manipulation task, resulting in reduced effective connectivity from SMG to AG (-0.45 Hz = A+B) during the task. Furthermore, the manipulation task weakened the connectivity from the semantic node FFG to the action node LOTC (-0.45 Hz, see **Figure 4b**).

None of the couplings between action nodes and semantic nodes were significantly modulated by the function or the value task according to the pre-defined FDR-corrected significance level of $p < 0.05$.

All mean coupling parameters across subjects for the intrinsic connections and their task-specific modulations of the winning model F4M2 are summarized in **Table III**.

Discussion

The current behavioral and functional imaging results confirm but also clearly extend previous findings on how action knowledge (here: manipulation knowledge) and semantic knowledge (here: function knowledge and value knowledge) about tools is processed in the human brain by exploring the effective connectivity of the underlying neural networks with the help of DCM (Grefkes and Fink, 2011). DCM analyses rest upon the results of the GLM analyses. The current GLM results are well in line with previous imaging studies on action and semantic knowledge about tools. Therefore, we here concentrate on the GLM results with direct relevance for the DCM analysis (please, see Supplementary material for a more detailed discussion of the activation patterns), and thereby focus the discussion on the novel effective connectivity results.

Brain regions processing action versus semantic knowledge about tools

As expected, the two tasks addressing semantic tool knowledge (function and value knowledge) led to similar activation patterns (see Results and Supplementary Material). Contrasting these semantic knowledge tasks with the action knowledge task revealed differential activations in the FFG and AG bilaterally and in the mPFC.

In the framework of the initial two stream-hypothesis (vision-for-perception (ventral stream) and vision-for-action (dorsal stream) (Goodale and Milner, 1992)), the FFG represents a region within the ventral visuo-motor stream (Chao, et al., 1999; Hutchison, et al., 2014; Mahon, et al., 2007), which, as a whole, supports the recognition of tools and their functions. Recently, Martin and colleagues associated lesions to areas within the ventral stream (here: ATL) with poorer performance in a tool selection task, similar to our tool function task (Martin, et al.,

2016a). Moreover, (bilateral) activations in the AG and FFG have been shown previously in numerous neuroimaging studies during semantic processing (Binder, et al., 2009; Chao, et al., 1999; Chen, et al., 2016; Price, et al., 2015; Rumiati, et al., 2004; Seghier, 2013; Zhang, et al., 2016). Note that the AG was activated by the semantic tasks and the SMG by the manipulation task, suggesting that these subdivisions of the (large) IPL presumably play different roles in the processing of tool knowledge or tool use (Martin, et al., 2016a; Randerath, et al., 2017). Finally, note that activation of the mPFC is in line with previous studies on valuation in healthy subjects (Domenech, et al., 2017) and particularly in estimating the monetary value of objects (Smith and Milner, 1984).

In contrast, the manipulation task led to activations in the left IPS, left SMG, left IFG and bilateral LOTC. The left IPS, SMG and IFG are parts of a left fronto-parietal network, hosting action representations. These regions are also activated in healthy subjects during actual tool-use (Binkofski, et al., 1999; Brandi, et al., 2014; Yoon, et al., 2012). The SMG and (a)IPS represent core regions of the ventro-dorsal stream (Binkofski and Buxbaum, 2013). Moreover, they are the putative site of parietal action representations (including the skilled actions associated with familiar objects). Lesions to these regions compromise those action representations and lead to impaired tool-use (Goldenberg and Spatt, 2009; Martin, et al., 2016a; Martin, et al., 2016c) and thus tool-use apraxia (Buxbaum, et al., 2000).

The bilateral activation of the LOTC during the manipulation task calls for further discussion. Overall, its activation concurs with the proposed role of the LOTC in action processing (Lingnau and Downing, 2015), and in particular, tool-knowledge and tool-associated hand actions (Bracci, et al., 2012; Perini, et al., 2014; Vingerhoets, 2008). Thus, LOTC lesions are associated with impaired action recognition (Tarhan, et al., 2015) and deficits in imitation and pantomime

of tool-use (Hoeren, et al., 2014). Nevertheless, it cannot be ruled out that the differential LOTC activation (encompassing EBA) may have – in part – been triggered by differences in visual stimuli (here: hands versus objects / money), since visual presentation of body parts and/ or tools activates partially overlapping regions in the LOTC (Bracci, et al., 2016; Bracci, et al., 2012; Gallivan, et al., 2013). Within the LOTC, the 'body-selective' EBA and the 'tool-selective' posterior MTG are both also involved in decoding the 'intention' to perform a motor act, i.e., the planning of hand- and tool-related actions (Gallivan, et al., 2016; Gallivan, et al., 2013; Zimmermann, et al., 2018). Such planning strategy of hand- and tool-related actions was presumably required to resolve the applied manipulation task. Consequently, the most parsimonious explanation for the current (large) bilateral LOTC activation encompassing MTG and EBA is a combination of differential stimulus-related activation (here: hands) and activation related to action processing (also see limitations).

Effective connectivity during the processing of action and semantic knowledge about tools

The current results shed light on the effective connectivity during processing of action knowledge and semantic knowledge about tools in the left hemisphere. In the DCM analysis, the dorsal regions (LOTC, IPS, SMG, IFG) that were activated in the action knowledge task were included as 'action nodes', and the ventral regions (FFG, AG, mPFC) activated in the semantic knowledge tasks were included as 'semantic nodes'.

 Note that the presence of similar activation patterns in the GLM analysis does not necessarily imply similar interregional connectivity. Thus, the V task was chosen as a further semantic task in addition to the F task to investigate whether the patterns of effective connectivity generalize across different aspects of semantic tool knowledge.

The winning model F4M2 revealed just one significant modulatory effect (p<0.05, FDR-corrected) for the V and the F tasks (see **Figure 4c** and **4d)**. Nevertheless, this finding is important as such a modulatory effect was found for both semantic tasks (V and F) in the same direction (from V1/2 to the FFG), same quality (positive, strengthening), and with similar strength (V: +0,5 Hz and F: +0.76 Hz). This indicates that different aspects of semantic knowledge about tools not only engage similar brain regions as reflected in activation patterns but also show coherent directed influences (effective connectivity) that one region exerts upon another. Further research is warranted to investigate the effective connectivity patterns for other semantic aspects of tool knowledge.

Moreover, we were specifically interested in the interactions between semantic nodes and action nodes that may reflect an information exchange during semantic and action processing. The finding of interregional bidirectional connections between action nodes and semantic nodes as observed in the winning model F4M2 (see **Suppl. Figure S1e**) corroborates the notion that areas processing semantic aspects of tools interact with the areas mediating action representations. In particular, the winning model featured bidirectional couplings between the semantic and action nodes (notably between FFG and LOTC as well as between AG and SMG). These effective connectivity findings are consistent with previous structural and functional connectivity studies. Anatomic studies revealed bidirectional connections between ventral and dorsal regions in the macaque (Borra, et al., 2008) and in humans (Takemura, et al., 2016). fMRI studies revealed functional connectivity between ventral areas and parietal action representations (Garcea and Mahon, 2014; Hutchison, et al., 2014).

However, to date, only few studies have addressed how context-dependent information about tools is exchanged between regions of the semantic and action system. Such studies have mostly focused on the putative role of ventral regions in contributing information about

tools to action representations. To this end, different methods were employed. For instance, some fMRI studies utilized the fact that parvocellular channels project principally to the ventral visual stream and not the dorsal visual stream and hence presented stimuli only 'visible' to ventral visual stream areas. Utilizing this method, these studies found subsequent transfer of information to parietal action representations – particularly between ventral tool-selective areas (left FFG and MTG) and the left IPL and IPS (Almeida, et al., 2013; Kristensen, et al., 2016; Mahon, et al., 2013). Further support for this notion was provided by Garcea and colleagues, who showed tool-selective left IPL responses irrespective of whether the tool stimuli were presented in the right or left visual field. This tool-selective parietal response that was resilient to contralateral visual field biases suggests that the left IPL received tool information from ventral regions (Garcea, et al., 2016). Recently, Chen and colleagues revealed with PPI (psychophysical interactions) and DCM that 'toolness' itself exhibited a strong modulation of connectivity between ventral areas (left LOTC extending into MTG) and parietal action representations (left IPS) (Chen, et al., 2017a). Interestingly, Zimmermann and colleagues lately revealed strong functional and structural connectivity of the EBA with the parietal cortex, suggesting a functional role of the EBA in the planning of goal-directed actions, possibly contributing information about adequate postural configurations for tool use (Zimmermann, et al., 2018).

In line with these studies, processing action knowledge in the context of our manipulation task led to a strengthening of connectivity from the left LOTC to the left parietal cortex (SMG), presumably hosting action representations (see **Figure 4b**). However, as some ambiguity exists about the causes of the current LOTC activations (encompassing posterior MTG and EBA, see discussion above and limitations), we refrain from making any specific inferences about the particular type of information exchange between left LOTC and left parietal cortex (SMG).

With respect to the functional role of the above described connections between ventral areas and parietal action representations, previous studies suggest that the retrieval of action knowledge (needed for adequate manipulation) relies – at least in part – on the identification of the tool (Garcea, et al., 2016; Hutchison, et al., 2014; Kristensen, et al., 2016; Mahon, et al., 2013). Alternatively, the particular contribution of the LOTC to the parietal action representations may involve action planning (Gallivan, et al., 2016; Gallivan, et al., 2013; Zimmermann, et al., 2018).

While overall, models featuring couplings between semantic nodes and action nodes were superior to the other models, the model parameters indicated a weakening of effective connectivity between FFG and LOTC during our manipulation task. In the same vein, connectivity from SMG (action node) to AG (semantic node) was also weakened. This relative weakening of the effective connectivity between action and semantic nodes in the context of our manipulation task might have facilitated the evaluation of different feasible hand configurations for interacting with a given tool (supported by the action nodes) irrespective of the identification of the tool (processed by the semantic nodes). Note that a recent fMRI study (Hutchison and Gallivan, 2016) did not reveal significant functional connectivity between ventral areas and action representations during sensori-motor and visual-perceptual tasks. At first sight, these findings seem at odds with the theory that action representations are contingent on semantic processing (Almeida, et al., 2013; Chen, et al., 2017a; Garcea, et al., 2016; Kristensen, et al., 2016; Mahon, et al., 2013). However, an alternative hypothesis claims that – to some extent – object perception can also be mediated via the dorsal pathway (for a detailed review on this notion see Freud et al., 2016). In a similar vein, neural activity patterns related to motor-relevant object properties were found in ventral stream areas (Gallivan, et al., 2013; Mahon, et al., 2007), providing evidence that the ventral stream is

modulated by motor attributes contributing to object recognition (Sim, et al., 2015). These findings clearly challenge a strict functional segregation of processing semantic aspects and action representations of tools.

Interestingly, while connectivity between action and semantic nodes was weakened, a relative strengthening of information transmission from more caudal to more rostral action nodes was revealed (V1/2→LOTC→IPS→SMG→IFG), while the connections were weakened in the reverse direction (IFG→SMG→IPS→LOTC) suggesting a predominantly caudo-rostral information flow within the fronto-parietal tool network.

Limitations

It might be argued that the differences between the manipulation knowledge task on the one side and the function and value knowledge tasks on the other side are related to increased difficulty in processing the hand postures. However, previous studies analogously reported longer RTs for manipulation tasks compared to function tasks (Evans, et al., 2016) – some even without the presentation of hands (Garcea and Mahon, 2012) – suggesting different cognitive processing strategies rather than mere differences in task difficulty. In the same vein, similar activation patterns were found in imaging studies of action knowledge, which did not use hand pictures as visual stimuli (Assmus, et al., 2007; Chen, et al., 2016; Kellenbach, et al., 2003; Vingerhoets, 2008). Furthermore, computation of term-based automatic meta-analyses with the database Neurosynth (http://neurosynth.org) revealed highly similar bilateral activations in the LOTC for the terms 'body' or 'hands' (based on 443 studies for 'body' and 104 studies for 'hands'). Importantly, however, the term 'actions' (currently based on 501 studies) also revealed bilateral LOTC activations. Moreover, the current large bilateral LOTC activations (for

the contrast 2*M>(F+V)) fully encompassed the Neurosynth results for 'hands' and 'body' as well as those for 'actions'. Thus, the mere fact that there are bilateral activations in the LOTC does not necessarily imply that these are driven by visual stimuli (here: body parts/hands), since action processing also leads to bilateral LOTC activations. This renders it unlikely that the current activations for processing of action knowledge can be solely attributed to differences in visual stimuli.

Taking into account that dysfunction of the anterior temporal lobe (ATL) caused by stroke (Martin, et al., 2016a) or neurodegeneration (Hodges, et al., 2000) leads to pronounced deficits in function knowledge about tools, and that rTMS over the ATL led to longer RTs for functional judgments (Ishibashi, et al., 2011), the absence of significant ATL activation in the current study during the function knowledge task may be considered unexpected. However, neuroimaging studies do not consistently show ATL activation during semantic tasks (Rice, et al., 2015; Visser, et al., 2010). The absence of ATL activation in our study might be due to a methodical limitation, since optimal BOLD imaging of the ATL requires the dual gradient-echo method (Halai, et al., 2014). Adopting this method, Jackson and colleagues could recently show that within the semantic network, the ATL showed functional connectivity with the mPFC and the AG, which were significantly activated in the current function and value knowledge tasks tapping on semantic tool knowledge (Jackson, et al., 2016). Further studies combining the current DCM approach with dual gradient-echo imaging are warranted to shed further light on the *effective* connectivity of the ATL within the network supporting conceptual knowledge about tools.

Conclusion

Effective connectivity analyses with DCM revealed interregional bidirectional connectivity in the networks processing action and semantic knowledge about tools as well as relevant couplings between action and semantic nodes.

The two semantic tasks (function and value knowledge) both significantly strengthened the connectivity from the visual cortex to the fusiform gyrus. As this modulation occurred in a coherent manner for both semantic tasks, these findings suggest that different aspects of semantic tool knowledge are not only processed in similar brain regions, but that these brain regions also show similar interregional effective connectivity during this processing.

The most pronounced modulatory effects of effective connectivity patterns were observed for the action knowledge task with a predominantly caudo-rostral information flow within the parieto-frontal action network.

While our effective connectivity results certainly contribute to the understanding of how tool knowledge is processed in the human brain, further research is warranted to characterize the effective connectivity during actual tool use and disturbed connectivity patterns between semantic and action nodes in patients suffering from apraxia or semantic dementia.

All authors state that there are no conflicts of interest.

References

Almeida J, Fintzi AR, Mahon BZ (2013): Tool manipulation knowledge is retrieved by way of the ventral visual object processing pathway. Cortex 49:2334-44.

Andres M, Pelgrims B, Olivier E (2013): Distinct contribution of the parietal and temporal cortex to hand configuration and contextual judgements about tools. Cortex 49:2097-105.

Ashburner J, Friston KJ (2005): Unified segmentation. Neuroimage 26:839-51.

Assmus A, Giessing C, Weiss PH, Fink GR (2007): Functional interactions during the retrieval of conceptual action knowledge: an fMRI study. Journal of cognitive neuroscience 19:1004-12.

Baumard J, Lesourd M, Remigereau C, Jarry C, Etcharry-Bouyx F, Chauvire V, Osiurak F, Le Gall D (2017): Tool use in neurodegenerative diseases: Planning or technical reasoning? J Neuropsychol.

Benjamini Y, Hochberg Y (1995): Controlling the False Discovery Rate: A Practical and Powerful Approach to Multiple Testing. Journal of the Royal Statistical Society. Series B (Methodological) 57:289-300.

Binder JR, Desai RH, Graves WW, Conant LL (2009): Where is the semantic system? A critical review and meta-analysis of 120 functional neuroimaging studies. Cereb Cortex 19:2767-96.

Binkofski F, Buccino G, Stephan KM, Rizzolatti G, Seitz RJ, Freund HJ (1999): A parieto-premotor network for object manipulation: evidence from neuroimaging. Exp Brain Res 128:210-3.

Binkofski F, Buxbaum LJ (2013): Two action systems in the human brain. Brain Lang 127:222-9.

Boronat CB, Buxbaum LJ, Coslett HB, Tang K, Saffran EM, Kimberg DY, Detre JA (2005): Distinctions between manipulation and function knowledge of objects: evidence from functional magnetic resonance imaging. Brain research. Cognitive brain research 23:361-73.

Borra E, Belmalih A, Calzavara R, Gerbella M, Murata A, Rozzi S, Luppino G (2008): Cortical connections of the macaque anterior intraparietal (AIP) area. Cereb Cortex 18:1094-111.

Bracci S, Cavina-Pratesi C, Connolly JD, Ietswaart M (2016): Representational content of occipitotemporal and parietal tool areas. Neuropsychologia 84:81-8.

Bracci S, Cavina-Pratesi C, Ietswaart M, Caramazza A, Peelen MV (2012): Closely overlapping responses to tools and hands in left lateral occipitotemporal cortex. J Neurophysiol 107:1443-56.

Brandi ML, Wohlschlager A, Sorg C, Hermsdorfer J (2014): The neural correlates of planning and executing actual tool use. J Neurosci 34:13183-94.

Buxbaum LJ, Giovannetti T, Libon D (2000): The role of the dynamic body schema in praxis: evidence from primary progressive apraxia. Brain Cogn 44:166-91.

Buxbaum LJ, Kalenine S (2010): Action knowledge, visuomotor activation, and embodiment in the two action systems. Annals of the New York Academy of Sciences 1191:201-18.

Buxbaum LJ, Schwartz MF, Carew TG (1997): The Role of Semantic Memory in Object Use. Cognitive Neuropsychology 14:219-254.

Canessa N, Borgo F, Cappa SF, Perani D, Falini A, Buccino G, Tettamanti M, Shallice T (2008): The different neural correlates of action and functional knowledge in semantic memory: an FMRI study. Cereb Cortex 18:740-51.

Carey DP, Harvey M, Milner AD (1996): Visuomotor sensitivity for shape and orientation in a patient with visual form agnosia. Neuropsychologia 34:329-37.

Chao LL, Haxby JV, Martin A (1999): Attribute-based neural substrates in temporal cortex for perceiving and knowing about objects. Nature neuroscience 2:913-9.

Chen J, Snow JC, Culham JC, Goodale MA (2017a): What Role Does "Elongation" Play in "Tool-Specific" Activation and Connectivity in the Dorsal and Ventral Visual Streams? Cereb Cortex:1-15.

Chen Q, Garcea FE, Jacobs RA, Mahon BZ (2017b): Abstract Representations of Object-Directed Action in the Left Inferior Parietal Lobule. Cereb Cortex:1-13.

Chen Q, Garcea FE, Mahon BZ (2016): The Representation of Object-Directed Action and Function Knowledge in the Human Brain. Cereb Cortex 26:1609-18.

Coccia M, Bartolini M, Luzzi S, Provinciali L, Ralph MA (2004): Semantic memory is an amodal, dynamic system: Evidence from the interaction of naming and object use in semantic dementia. Cogn Neuropsychol 21:513-27.

Daunizeau J, David O, Stephan KE (2011): Dynamic causal modelling: a critical review of the biophysical and statistical foundations. Neuroimage 58:312-22.

De Renzi E, Lucchelli F (1988): Ideational apraxia. Brain 111 (Pt 5):1173-85.

Domenech P, Redoute J, Koechlin E, Dreher JC (2017): The Neuro-Computational Architecture of Value-Based Selection in the Human Brain. Cereb Cortex.

Eickhoff SB, Stephan KE, Mohlberg H, Grefkes C, Fink GR, Amunts K, Zilles K (2005): A new SPM toolbox for combining probabilistic cytoarchitectonic maps and functional imaging data. Neuroimage 25:1325-35.

Eklund A, Nichols TE, Knutsson H (2016): Cluster failure: Why fMRI inferences for spatial extent have inflated false-positive rates. Proc Natl Acad Sci U S A 113:7900-5.

Evans C, Edwards MG, Taylor LJ, Ietswaart M (2016): Perceptual decisions regarding object manipulation are selectively impaired in apraxia or when tDCS is applied over the left IPL. Neuropsychologia 86:153-66.

Freud E, Plaut DC, Behrmann M (2016): 'What' Is Happening in the Dorsal Visual Pathway. Trends Cogn Sci 20:773-84.

Friston KJ, Harrison L, Penny W (2003): Dynamic causal modelling. Neuroimage 19:1273-302.

Friston KJ, Penny WD, Glaser DE (2005): Conjunction revisited. Neuroimage 25:661-7.

Gallivan JP, Johnsrude IS, Flanagan JR (2016): Planning Ahead: Object-Directed Sequential Actions Decoded from Human Frontoparietal and Occipitotemporal Networks. Cereb Cortex 26:708-30.

Gallivan JP, McLean DA, Valyear KF, Culham JC (2013): Decoding the neural mechanisms of human tool use. eLife 2:e00425.

Garcea FE, Kristensen S, Almeida J, Mahon BZ (2016): Resilience to the contralateral visual field bias as a window into object representations. Cortex 81:14-23.

Garcea FE, Mahon BZ (2012): What is in a tool concept? Dissociating manipulation knowledge from function knowledge. Mem Cognit 40:1303-13.

Garcea FE, Mahon BZ (2014): Parcellation of left parietal tool representations by functional connectivity. Neuropsychologia 60:131-43.

Goldenberg G, Spatt J (2009): The neural basis of tool use. Brain 132:1645-55.

Goodale MA, Milner AD (1992): Separate visual pathways for perception and action. Trends in neurosciences 15:20-5.

Grefkes C, Fink GR (2005): The functional organization of the intraparietal sulcus in humans and monkeys. Journal of anatomy 207:3-17.

Grefkes C, Fink GR (2011): Reorganization of cerebral networks after stroke: new insights from neuroimaging with connectivity approaches. Brain 134:1264-76.

Halai AD, Welbourne SR, Embleton K, Parkes LM (2014): A comparison of dual gradient-echo and spin-echo fMRI of the inferior temporal lobe. Hum Brain Mapp 35:4118-28.

Hodges JR, Bozeat S, Lambon Ralph MA, Patterson K, Spatt J (2000): The role of conceptual knowledge in object use evidence from semantic dementia. Brain 123 (Pt 9):1913-25.

Hodges JR, Spatt J, Patterson K (1999): "What" and "how": evidence for the dissociation of object knowledge and mechanical problem-solving skills in the human brain. Proc Natl Acad Sci U S A 96:9444-8.

Hoeren M, Kummerer D, Bormann T, Beume L, Ludwig VM, Vry MS, Mader I, Rijntjes M, Kaller CP, Weiller C (2014): Neural bases of imitation and pantomime in acute stroke patients: distinct streams for praxis. Brain 137:2796-810.

Hutchison RM, Culham JC, Everling S, Flanagan JR, Gallivan JP (2014): Distinct and distributed functional connectivity patterns across cortex reflect the domain-specific constraints of object, face, scene, body, and tool category-selective modules in the ventral visual pathway. Neuroimage 96:216-36.

Hutchison RM, Gallivan JP (2016): Functional coupling between frontoparietal and occipitotemporal pathways during action and perception. Cortex.

Ishibashi R, Lambon Ralph MA, Saito S, Pobric G (2011): Different roles of lateral anterior temporal lobe and inferior parietal lobule in coding function and manipulation tool knowledge: evidence from an rTMS study. Neuropsychologia 49:1128-35.

Ishibashi R, Mima T, Fukuyama H, Pobric G (2017): Facilitation of Function and Manipulation Knowledge of Tools Using Transcranial Direct Current Stimulation (tDCS). Front Integr Neurosci 11:37.

Jackson RL, Hoffman P, Pobric G, Lambon Ralph MA (2016): The Semantic Network at Work and Rest: Differential Connectivity of Anterior Temporal Lobe Subregions. J Neurosci 36:1490-501.

Kellenbach ML, Brett M, Patterson K (2003): Actions speak louder than functions: the importance of manipulability and action in tool representation. Journal of cognitive neuroscience 15:30-46.

Kristensen S, Garcea FE, Mahon BZ, Almeida J (2016): Temporal Frequency Tuning Reveals Interactions between the Dorsal and Ventral Visual Streams. Journal of cognitive neuroscience 28:1295-302.

Lauro-Grotto R, Piccini C, Shallice T (1997): Modality-specific operations in semantic dementia. Cortex 33:593-622.

Lingnau A, Downing PE (2015): The lateral occipitotemporal cortex in action. Trends Cogn Sci 19:268-77.

Magnie MN, Ferreira CT, Giusiano B, Poncet M (1999): Category specificity in object agnosia: preservation of sensorimotor experiences related to objects. Neuropsychologia 37:67-74.

Mahon BZ, Kumar N, Almeida J (2013): Spatial frequency tuning reveals interactions between the dorsal and ventral visual systems. Journal of cognitive neuroscience 25:862-71.

Mahon BZ, Milleville SC, Negri GA, Rumiati RI, Caramazza A, Martin A (2007): Action-related properties shape object representations in the ventral stream. Neuron 55:507-20.

Martin M, Beume L, Kummerer D, Schmidt CS, Bormann T, Dressing A, Ludwig VM, Umarova RM, Mader I, Rijntjes M, Kaller CP, Weiller C (2016a): Differential Roles of Ventral and Dorsal Streams for Conceptual and Production-Related Components of Tool Use in Acute Stroke Patients. Cereb Cortex 26:3754-71.

Martin M, Dressing A, Bormann T, Schmidt CS, Kummerer D, Beume L, Saur D, Mader I, Rijntjes M, Kaller CP, Weiller C (2016b): Componental Network for the Recognition of Tool-Associated Actions: Evidence from Voxel-based Lesion-Symptom Mapping in Acute Stroke Patients. Cereb Cortex.

Martin M, Nitschke K, Beume L, Dressing A, Buhler LE, Ludwig VM, Mader I, Rijntjes M, Kaller CP, Weiller C (2016c): Brain activity underlying tool-related and imitative skills after major left hemisphere stroke. Brain 139:1497-516.

Mechelli A, Price CJ, Henson RN, Friston KJ (2003): Estimating efficiency a priori: a comparison of blocked and randomized designs. Neuroimage 18:798-805.

Milner AD (1997): Vision without knowledge. Philosophical transactions of the Royal Society of London. Series B, Biological sciences 352:1249-56.

Negri GA, Lunardelli A, Reverberi C, Gigli GL, Rumiati RI (2007): Degraded semantic knowledge and accurate object use. Cortex 43:376-88.

Nichols T, Brett M, Andersson J, Wager T, Poline JB (2005): Valid conjunction inference with the minimum statistic. Neuroimage 25:653-60.

Nichols T, Hayasaka S (2003): Controlling the familywise error rate in functional neuroimaging: a comparative review. Statistical methods in medical research 12:419-46.

Niessen E, Fink GR, Weiss PH (2014): Apraxia, pantomime and the parietal cortex. Neuroimage Clin 5:42-52.

Ochipa C, Rothi LJ, Heilman KM (1989): Ideational apraxia: a deficit in tool selection and use. Annals of neurology 25:190-3.

Penny WD, Stephan KE, Daunizeau J, Rosa MJ, Friston KJ, Schofield TM, Leff AP (2010): Comparing families of dynamic causal models. PLoS Comput Biol 6:e1000709.

Penny WD, Stephan KE, Mechelli A, Friston KJ (2004): Comparing dynamic causal models. Neuroimage 22:1157-72.

Perini F, Caramazza A, Peelen MV (2014): Left occipitotemporal cortex contributes to the discrimination of tool-associated hand actions: fMRI and TMS evidence. Frontiers in human neuroscience 8:591.

Price AR, Bonner MF, Peelle JE, Grossman M (2015): Converging evidence for the neuroanatomic basis of combinatorial semantics in the angular gyrus. J Neurosci 35:3276-84.

Randerath J, Valyear KF, Philip BA, Frey SH (2017): Contributions of the parietal cortex to increased efficiency of planning-based action selection. Neuropsychologia 105:135-143.

Rice GE, Lambon Ralph MA, Hoffman P (2015): The Roles of Left Versus Right Anterior Temporal Lobes in Conceptual Knowledge: An ALE Meta-analysis of 97 Functional Neuroimaging Studies. Cereb Cortex 25:4374-91.

Rizzolatti G, Matelli M (2003): Two different streams form the dorsal visual system: anatomy and functions. Exp Brain Res 153:146-57.

Rumiati RI, Weiss PH, Shallice T, Ottoboni G, Noth J, Zilles K, Fink GR (2004): Neural basis of pantomiming the use of visually presented objects. Neuroimage 21:1224-31.

Sakreida K, Effnert I, Thill S, Menz MM, Jirak D, Eickhoff CR, Ziemke T, Eickhoff SB, Borghi AM, Binkofski F (2016): Affordance processing in segregated parieto-frontal dorsal stream sub-pathways. Neuroscience and biobehavioral reviews 69:89-112.

Seghier ML (2013): The angular gyrus: multiple functions and multiple subdivisions. The Neuroscientist : a review journal bringing neurobiology, neurology and psychiatry 19:43-61.

Sim EJ, Helbig HB, Graf M, Kiefer M (2015): When Action Observation Facilitates Visual Perception: Activation in Visuo-Motor Areas Contributes to Object Recognition. Cereb Cortex 25:2907-18.

Sirigu A, Duhamel JR, Poncet M (1991): The role of sensorimotor experience in object recognition. A case of multimodal agnosia. Brain 114 (Pt 6):2555-73.

Smith ML, Milner B (1984): Differential effects of frontal-lobe lesions on cognitive estimation and spatial memory. Neuropsychologia 22:697-705.

Stephan KE, Penny WD, Daunizeau J, Moran RJ, Friston KJ (2009a): Bayesian model selection for group studies. Neuroimage 46:1004-17.

Stephan KE, Penny WD, Moran RJ, den Ouden HE, Daunizeau J, Friston KJ (2010): Ten simple rules for dynamic causal modeling. Neuroimage 49:3099-109.

Stephan KE, Tittgemeyer M, Knosche TR, Moran RJ, Friston KJ (2009b): Tractography-based priors for dynamic causal models. Neuroimage 47:1628-38.

Takemura H, Rokem A, Winawer J, Yeatman JD, Wandell BA, Pestilli F (2016): A Major Human White Matter Pathway Between Dorsal and Ventral Visual Cortex. Cereb Cortex 26:2205-2214.

Tarhan LY, Watson CE, Buxbaum LJ (2015): Shared and Distinct Neuroanatomic Regions Critical for Tool-related Action Production and Recognition: Evidence from 131 Left-hemisphere Stroke Patients. Journal of cognitive neuroscience 27:2491-511.

Ungerleider LG, Mishkin M (1982): Two cortical visual systems. Analysis of visual behavior:549-586.

Vingerhoets G (2008): Knowing about tools: neural correlates of tool familiarity and experience. Neuroimage 40:1380-91.

Visser M, Jefferies E, Lambon Ralph MA (2010): Semantic processing in the anterior temporal lobes: a meta-analysis of the functional neuroimaging literature. Journal of cognitive neuroscience 22:1083-94.

Woo CW, Krishnan A, Wager TD (2014): Cluster-extent based thresholding in fMRI analyses: pitfalls and recommendations. Neuroimage 91:412-9.

Yoon EY, Humphreys GW, Kumar S, Rotshtein P (2012): The neural selection and integration of actions and objects: an fMRI study. Journal of cognitive neuroscience 24:2268-79.

Zhang W, Wang J, Fan L, Zhang Y, Fox PT, Eickhoff SB, Yu C, Jiang T (2016): Functional organization of the fusiform gyrus revealed with connectivity profiles. Hum Brain Mapp 37:3003-16.

Zimmermann M, Mars RB, de Lange FP, Toni I, Verhagen L (2018): Is the extrastriate body area part of the dorsal visuomotor stream? Brain Struct Funct 223:31-46.

Nina N. Kleineberg et al. – DCM analysis of tool knowledge

Figure legends

Figure 1. Experimental stimuli. This graphic shows examples of the experimental stimuli used drawing upon action tool knowledge and semantic tool knowledge. In the manipulation condition (M), the appropriate hand posture for manipulating the target tool (here: a hammer) had to be selected (here: the hand posture on the right side of the stimulus). In the function condition (F), subjects selected the appropriate recipient object for the target tool (here: the nail on the right side of the hammer). In the value knowledge condition (V), subjects estimated the monetary value of the target tool and selected the appropriate banknote or coin (here: the 10 Euro note on the left side of the stimulus). For a list of the 40 targets tools with the recipient objects (F) and respective coins/ banknotes (V), see Suppl. Table SIV.

Figure 2. Visual depiction of the results of the GLM analysis.

The activation patterns observed for the Manipulation>(Function+Value) contrast (red) and for the (Function+Value)>Manipulation contrast (blue) are projected onto a 3D surface rendering of a standard single subject brain. (**2a** view of left hemisphere, **2b** view from bottom, **2c** view from the front, **2d** view from behind)

Figure 3. Cluster of the individual coordinates used for DCM analysis.

Graphical demonstration of the individual MNI coordinates for the DCM analysis (listed in Suppl. Table SIII) projected onto a 3D surface rendering of a standard single subject brain. Regions of interest (ROIs): visual area 1 and 2 (V1/2) lateral occipito-temporal cortex (LOTC),

angular gyrus (AG), intraparietal sulcus (IPS), supramarginal gyrus (SMG), inferior frontal gyrus (IFG), medial prefrontal cortex (mPFC). All ROIs are in the *left* hemisphere. In this orientation not depicted: fusiform gyrus.

Figure 4. Effective Connectivity (DCM) Results

The *left*-hemispheric regions of interest considered in the DCM analysis are the visual area 1 and 2 (V1/2), lateral occipito-temporal cortex (LOTC), fusiform gyrus (FFG), angular gyrus (AG), intraparietal sulcus (IPS), supramarginal gyrus (SMG), inferior frontal gyrus (IFG), and medial prefrontal cortex (mPFC).

Significant effective connectivity is shown in quality (green = positive connectivity/ strengthening and red = negative connectivity/ weakening) and quantity (coupling strength in Hz (1/s)), gray = non-significant connectivity/ modulation (p<0.05, FDR-corrected).

Figure 4a. Intrinsic connectivity (A-Matrix).

Figure 4b,c,d. Modulation of the connectivity by the experimental tasks (B-Matrices). The modulations are the dynamic change of the A-matrix (Fig. 4a) during the tasks. The three experimental conditions consist of the Manipulation knowledge task (M, Fig. 4b), the Value knowledge task (V, Fig. 4c) and the Function knowledge task (F, Fig. 4d).

Supplementary figure legends

Suppl. Figure S1. Graphical presentation of all considered models.

Regions of interest: V1/2, visual area 1 and 2; LOTC, lateral occipito-temporal cortex; FFG, fusiform gyrus; AG, angular gyrus; IPS, intraparietal sulcus; SMG, supramarginal gyrus; IFG, inferior frontal gyrus; mPFC, medial prefrontal cortex (all ROIs are in the *left* hemisphere)

Experimental conditions: M, manipulation knowledge task; F, function knowledge task; V, value knowledge task.

Suppl. Figure S1a. Graphical presentation of all considered model families. Families differed in equipped intrinsic connections (A-matrix) with respect to putative *interactions* between semantic nodes and action nodes: F1, no interaction; F2, interaction within the occipito-temporal lobe (FFG–LOTC); F3, interaction within the parietal lobe, (AG–SMG); and F4, interactions within both, the occipito-temporal and the parietal lobe (FFG–LOTC, AG–SMG).

Suppl. Figure S1b.-e. Graphical presentation of all considered single models of the families.

Single models within a family differ in equipped modulatory effects by the experimental tasks (B-matrices). Three different levels of modulations were assumed; (i) modulatory effects throughout the occipito-temporal lobe only (V1/2, LOTC, FFG); (ii) modulatory effects throughout the occipito-temporal lobe and parietal lobe (V1/2, LOTC, FFG, IPS, SMG, AG); and (iii) modulatory effects at all (three) levels, i.e., throughout the occipito-temporal lobe, the parietal lobe and the frontal lobe (V1/2, LOTC, FFG, SMG, AG, IFG, mPFC). All these different hypotheses were configured as (a) unidirectional and (b) bidirectional. Accordingly, the investigated aspects led to a total of 24 models: four model families (F1 – F4, different interactions between action nodes and semantic nodes) with six models each (six = three (different levels of modulation) times two (unidirectional versus bidirectional)).

Supplementary material:

Supplement to the Results of the Functional Imaging GLM analysis

Action knowledge (Manipulation task) and Semantic knowledge (Function and Value task)

Comparing the manipulation task with either the function or the value knowledge task (M>F and M>V) revealed similar activation patterns (see **Supp. Table SI**): bilateral activations in the LOTC (comprising the extra-striate body area, EBA) and the left IPS. In addition, M>V yielded activation clusters in the left IFG, the SMG, and the left superior occipital gyrus. In contrast, the function task compared to the manipulation task (F>M) led to stronger activations in the FFG bilaterally, as well as in the mPFC. Contrasting V>M revealed activations in the right AG and in the mPFC. Finally, contrasting the value knowledge with the function knowledge (F>V) revealed no significant results, while the opposite contrast (F>V) led to a rather diffuse activation pattern including extra-striate cortex, left middle occipital gyrus, left FFG, and right insula (see **Suppl. Table I**). Note that the conjunction analysis of the contrasts F>M and V>M affirmed the common involvement of brain regions in the processing of the two semantic tool knowledge tasks (F and V), showing activations in the right FFG, extending into the extra-striate cortex, the AG bilaterally, the medial prefrontal cortex, and the primary visual area (see **Suppl. Table SII**).

For the results of the direct (superordinate) comparison of action knowledge and semantic knowledge about tools, on which the DCM analysis is based, please see manuscript.

Supplement to the Discussion regarding the fronto-parietal activation patterns of the manipulation task.

The observed activations in the parietal lobe (left IPS and left SMG) during the manipulation task are in line with various fMRI studies on action knowledge (Binder, et al., 2009; Bracci, et al., 2016; Canessa, et al., 2008; Vingerhoets, 2008; Vingerhoets, et al., 2013; Yoon, et al., 2012) and behavioral studies with non-invasive brain stimulation applied above the parietal lobe (Andres, et al., 2013; Evans, et al., 2016; Ishibashi, et al., 2011). In a fMRI study by Vingerhoets (2008), stronger activation in the SMG was revealed during the processing of familiar tools (stored manipulation knowledge) compared to unfamiliar tools (no stored manipulation knowledge) and thereby corroborated the notion that the SMG serves as a storage of tool-related action knowledge (for discussion of alternative theories regarding the SMG in object manipulation, see (Lesourd, et al., 2017)).

The activation of the left IFG, in particular BA 44, during the manipulation task is in good accordance with previous imaging studies on object use, action observation, action execution, and imitation (Caspers, et al., 2010; Chong, et al., 2008; Hamzei, et al., 2016; Hoeren, et al., 2013; Koechlin and Jubault, 2006) and, converging with our results, in matching of hand postures (Vingerhoets, et al., 2013).

Suppl. Table SI
Brain regions showing significant relative increases of BOLD response associated with each comparison of interest.

Suppl. Table SII
Brain regions showing significant relative increases of BOLD response associated with the Conjunction of Function > Manipulation and Value > Manipulation

Suppl. Table SIII
Individual coordinates used for time series extraction as well as the corresponding group maxima from the GLM analysis of the left hemisphere.

Suppl. Table SIV
List of the 40 target tools (in alphabetical order) together with the (recipient) objects used in Function knowledge (F) task and the respective coins and banknotes in the Value knowledge (V) task.

Suppl. Figure S1
Graphical presentation of all considered models.
Suppl. Figure S1a. **Graphical presentation of all considered model families.**
Suppl. Figure S1b.-e. **Graphical presentation of all considered single models of the families.**

Literature

Andres M, Pelgrims B, Olivier E (2013): Distinct contribution of the parietal and temporal cortex to hand configuration and contextual judgements about tools. Cortex 49:2097-105.

Binder JR, Desai RH, Graves WW, Conant LL (2009): Where is the semantic system? A critical review and meta-analysis of 120 functional neuroimaging studies. Cereb Cortex 19:2767-96.

Bracci S, Cavina-Pratesi C, Connolly JD, Ietswaart M (2016): Representational content of occipitotemporal and parietal tool areas. Neuropsychologia 84:81-8.

Canessa N, Borgo F, Cappa SF, Perani D, Falini A, Buccino G, Tettamanti M, Shallice T (2008): The different neural correlates of action and functional knowledge in semantic memory: an FMRI study. Cereb Cortex 18:740-51.

Caspers S, Zilles K, Laird AR, Eickhoff SB (2010): ALE meta-analysis of action observation and imitation in the human brain. Neuroimage 50:1148-67.

Chong TT, Williams MA, Cunnington R, Mattingley JB (2008): Selective attention modulates inferior frontal gyrus activity during action observation. Neuroimage 40:298-307.

Evans C, Edwards MG, Taylor LJ, Ietswaart M (2016): Perceptual decisions regarding object manipulation are selectively impaired in apraxia or when tDCS is applied over the left IPL. Neuropsychologia 86:153-66.

Hamzei F, Vry MS, Saur D, Glauche V, Hoeren M, Mader I, Weiller C, Rijntjes M (2016): The Dual-Loop Model and the Human Mirror Neuron System: an Exploratory Combined fMRI and DTI Study of the Inferior Frontal Gyrus. Cereb Cortex 26:2215-24.

Hoeren M, Kaller CP, Glauche V, Vry MS, Rijntjes M, Hamzei F, Weiller C (2013): Action semantics and movement characteristics engage distinct processing streams during the observation of tool use. Exp Brain Res 229:243-60.

Ishibashi R, Lambon Ralph MA, Saito S, Pobric G (2011): Different roles of lateral anterior temporal lobe and inferior parietal lobule in coding function and manipulation tool knowledge: evidence from an rTMS study. Neuropsychologia 49:1128-35.

Koechlin E, Jubault T (2006): Broca's area and the hierarchical organization of human behavior. Neuron 50:963-74.

Vingerhoets G (2008): Knowing about tools: neural correlates of tool familiarity and experience. Neuroimage 40:1380-91.

Vingerhoets G, Nys J, Honore P, Vandekerckhove E, Vandemaele P (2013): Human left ventral premotor cortex mediates matching of hand posture to object use. PLoS One 8:e70480.

Yoon EY, Humphreys GW, Kumar S, Rotshtein P (2012): The neural selection and integration of actions and objects: an fMRI study. Journal of cognitive neuroscience 24:2268-79.

Action tool knowledge

Semantic tool knowledge

Manipulation knowledge task (M)

Function knowledge task (F)

Value knowledge task (V)

Kleineberg et al. - Figure 1

Visual depiction of the GLM results

a.

b.

c.

d.

Kleineberg et al. - Figure 2
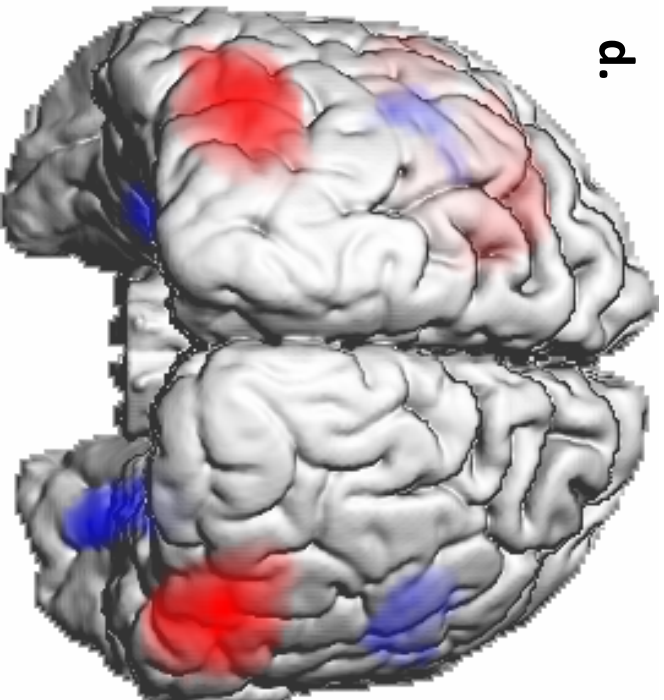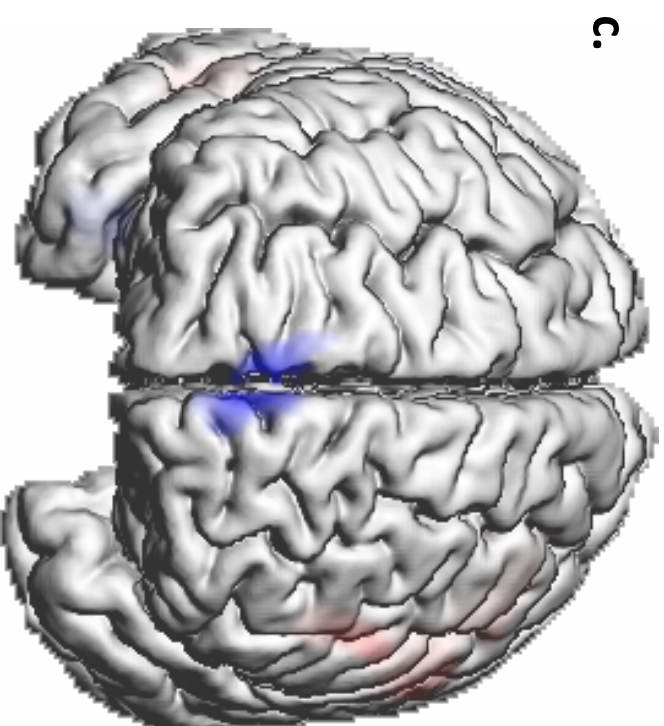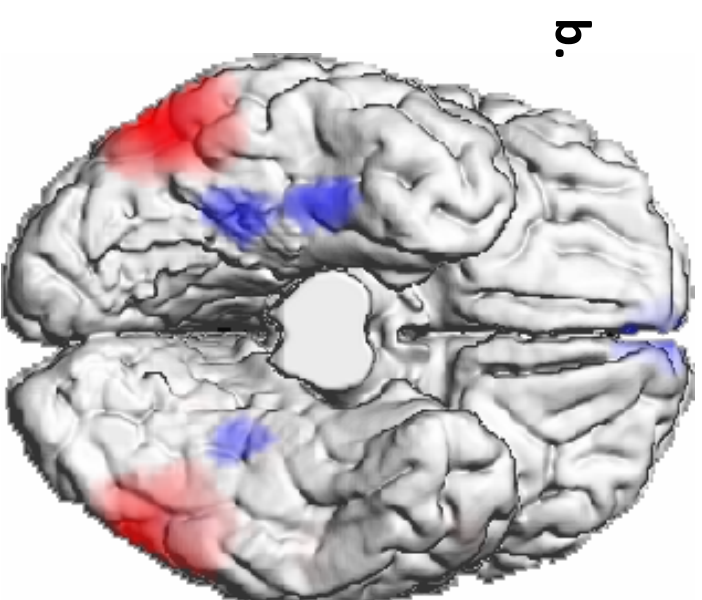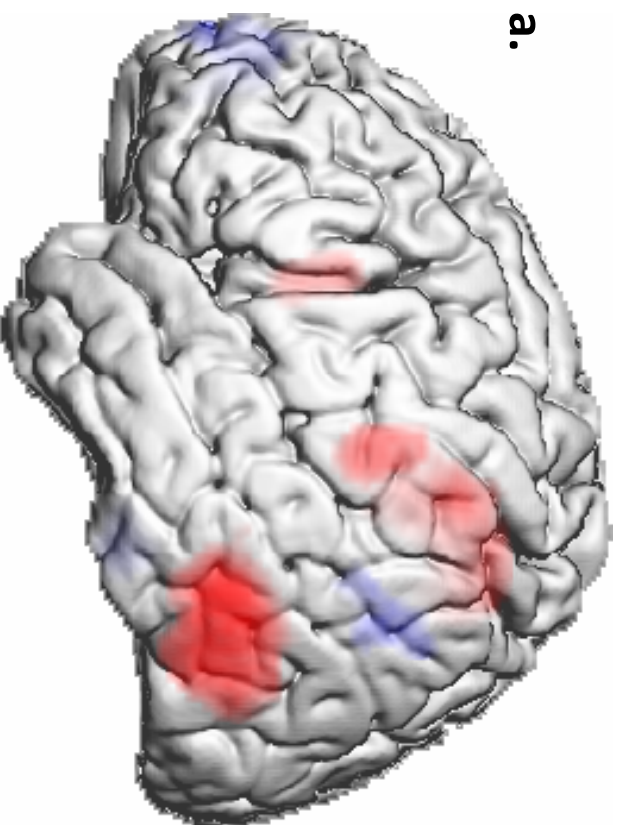
Cluster of the individual coordinates used for the DCM analysis

mPFC

IFG

SMG

IPS

LOTC

AG

V1/2

Kleineberg et al. - Figure 3
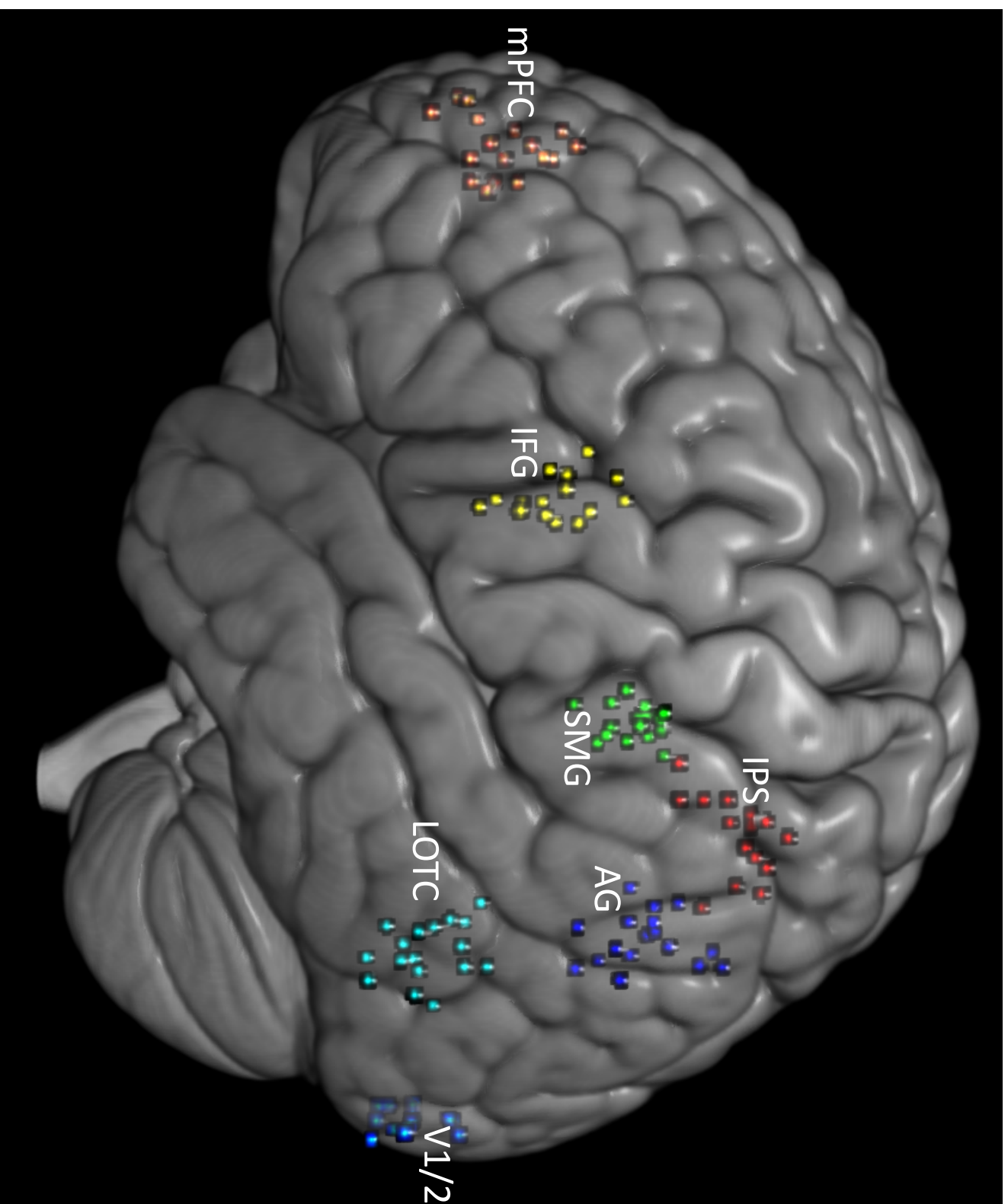
Effective Connectivity (DCM) Results

a.   Intrinsic connectivity
(A-Matrix)
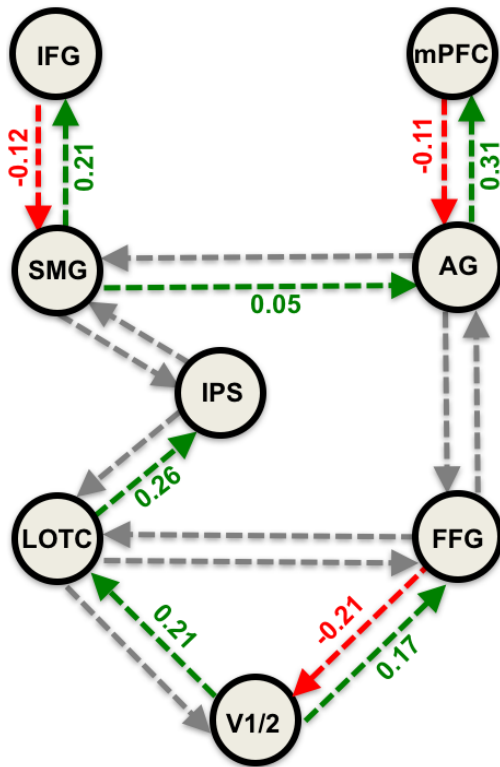
b.   Modulation by Manipulation task
(B-Matrix)
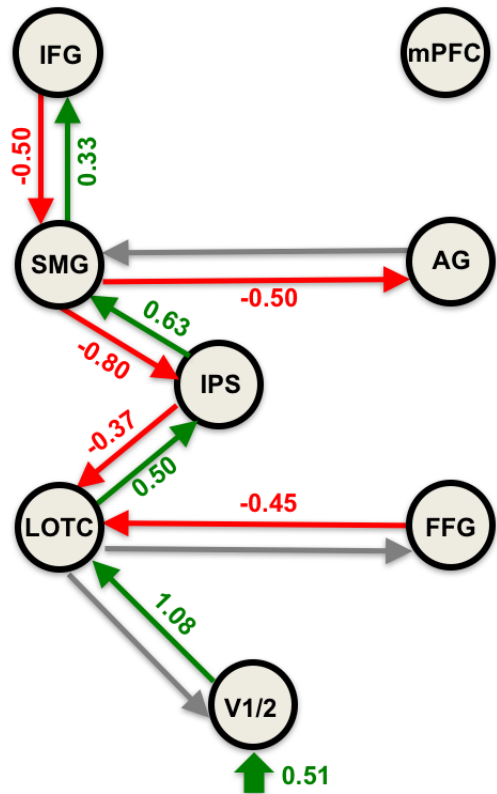
c.   Modulation by Value task
(B-Matrix)
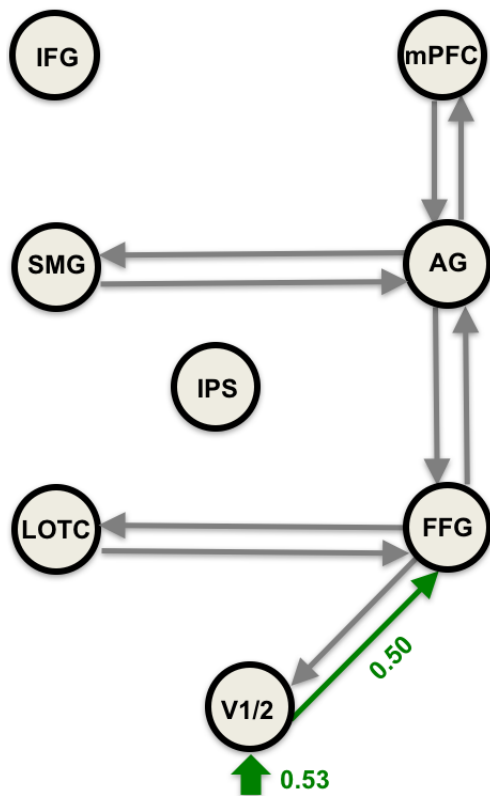
d.   Modulation by Function task
(B-Matrix)
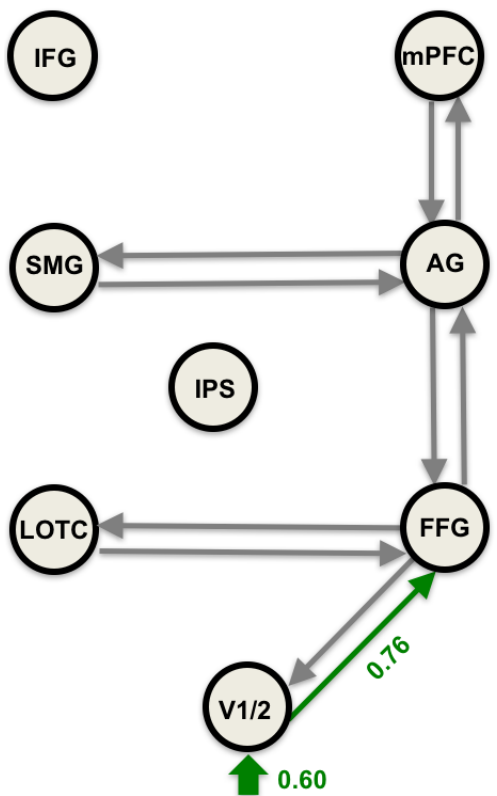
- - - / —— significant positive connectivity/ strengthening
- - - / —— significant negative connectivity/ weakening
- - - / —— non-significant connectivity/ modulation
⬆ direct input (C-Matrix)
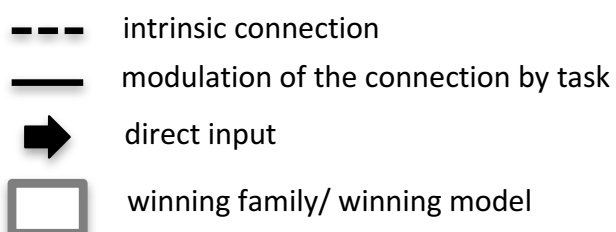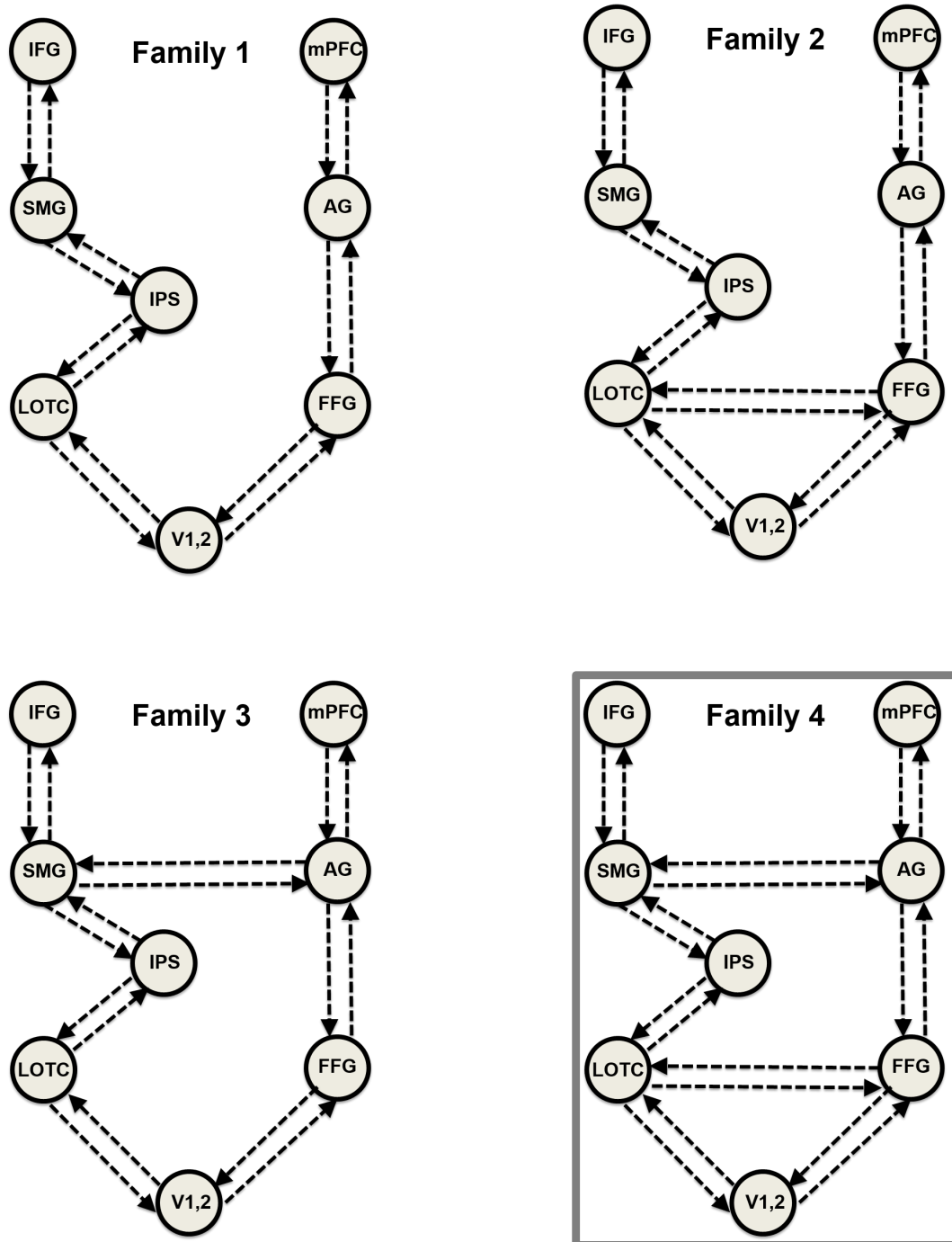
Kleineberg et al. - Figure 4

Graphical presentation of all considered model families

Kleineberg et al. - Suppl. Figure S1a.

Graphical presentation of all considered individual models of Family 1

Kleineberg et al. - Suppl. Figure S1b.

Graphical presentation of all considered individual models of Family 2

Kleineberg et al. - Suppl. Figure S1c.
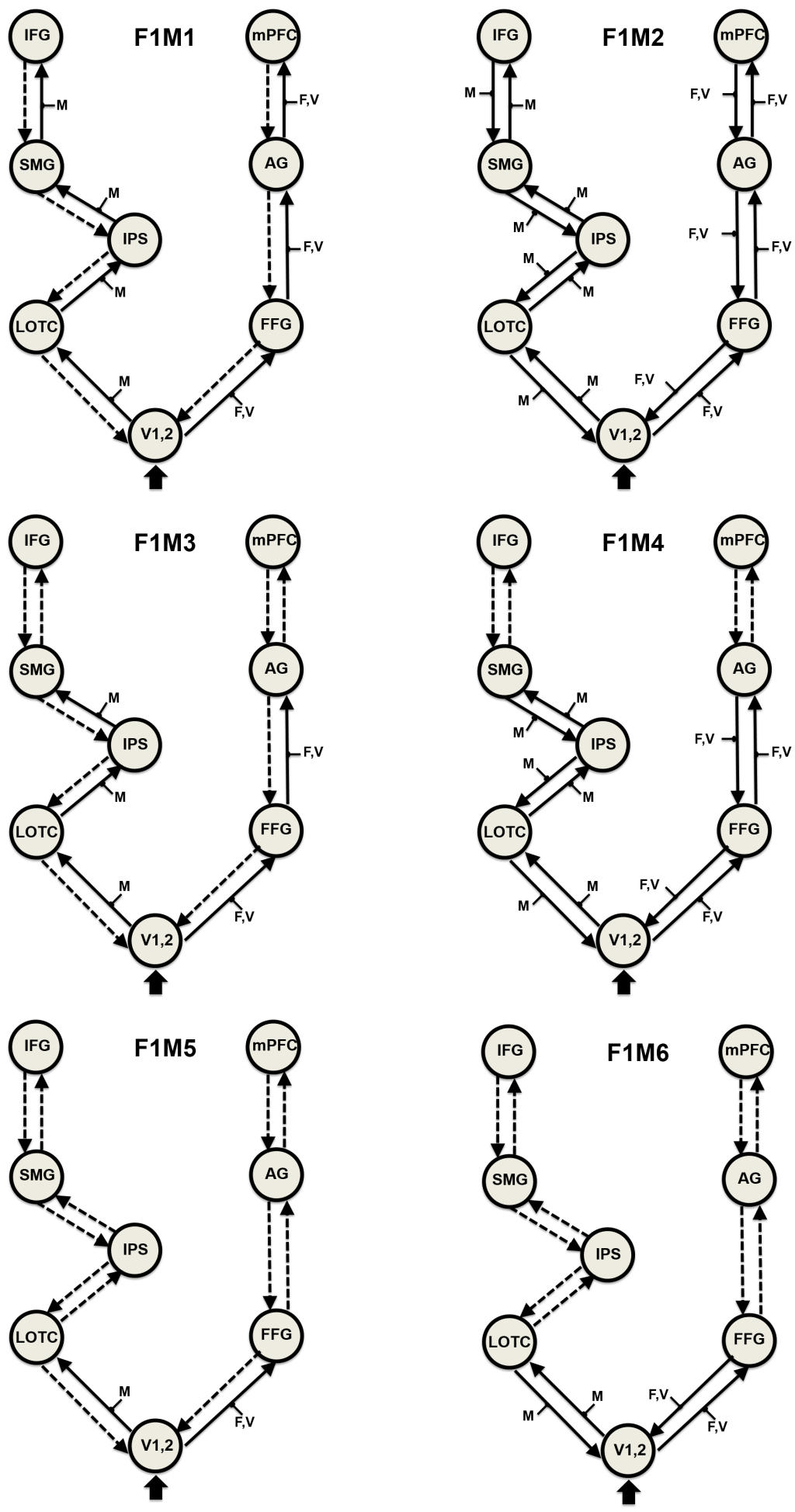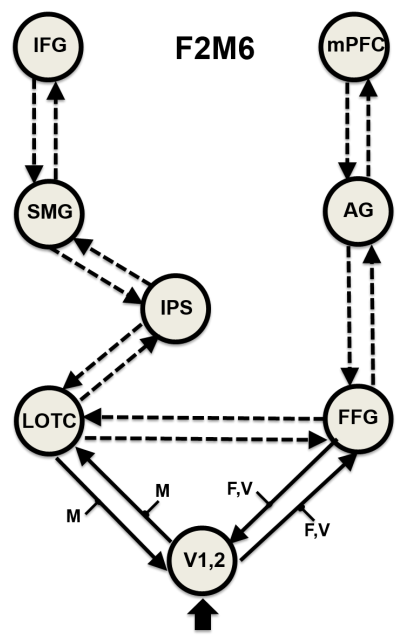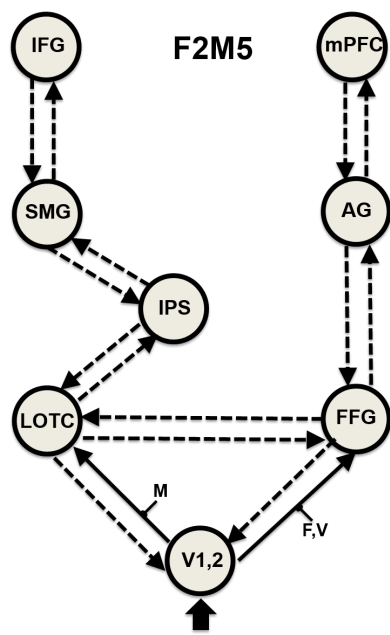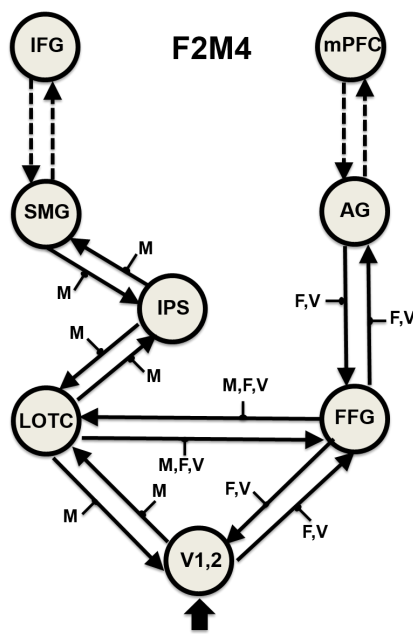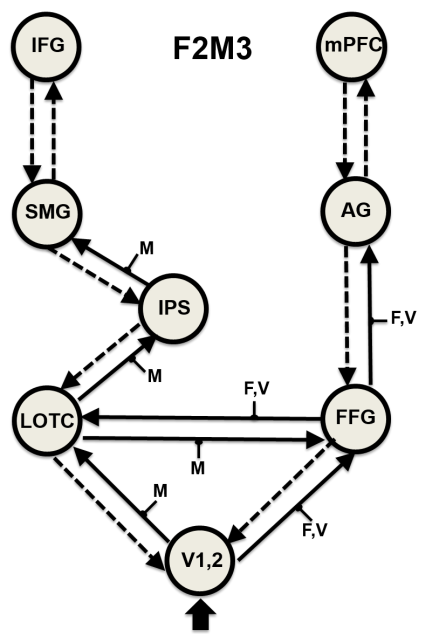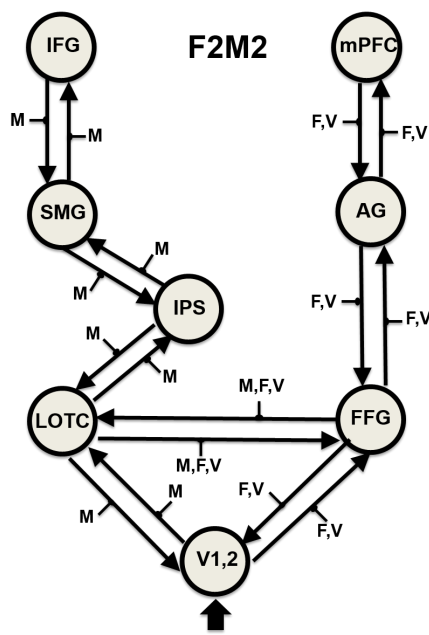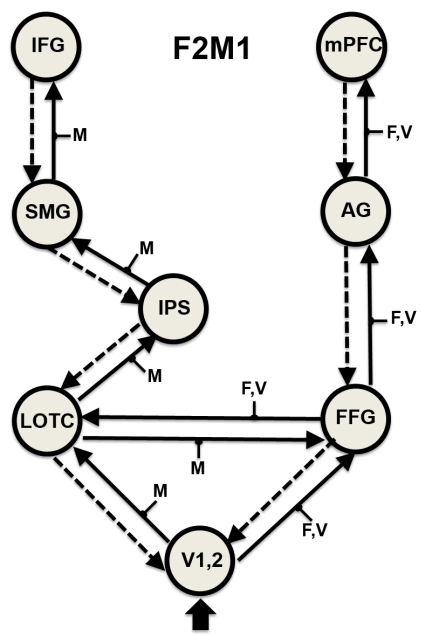
Graphical presentation of all considered individual models of Family 3

Graphical presentation of all considered individual models of Family 4

Kleineberg et al. - Suppl. Figure S1e.
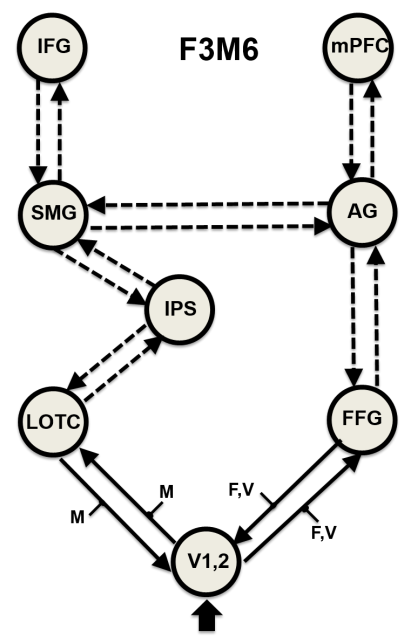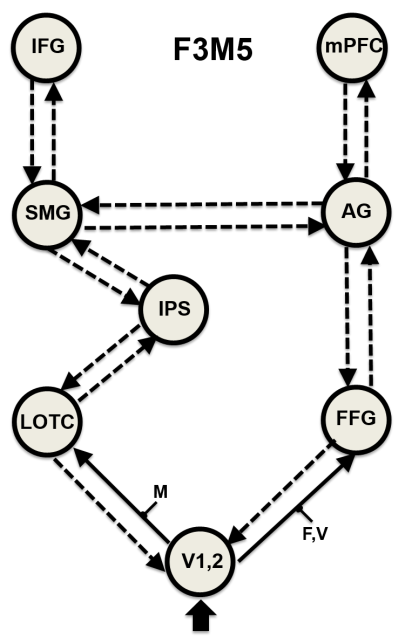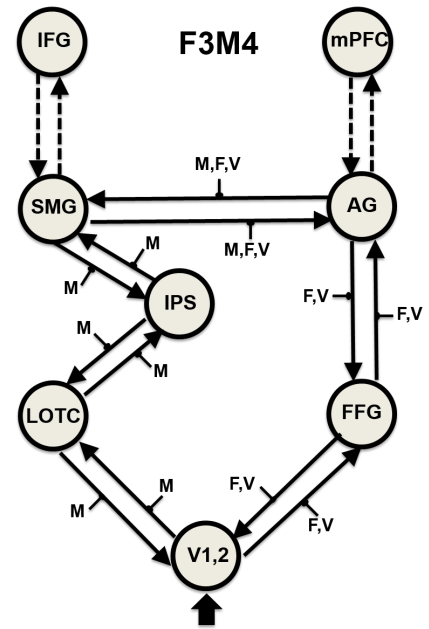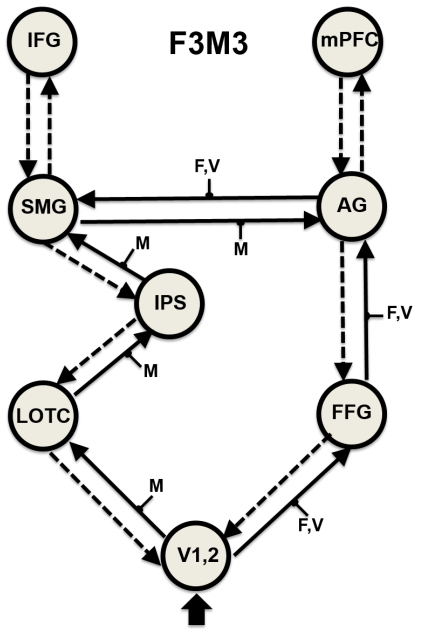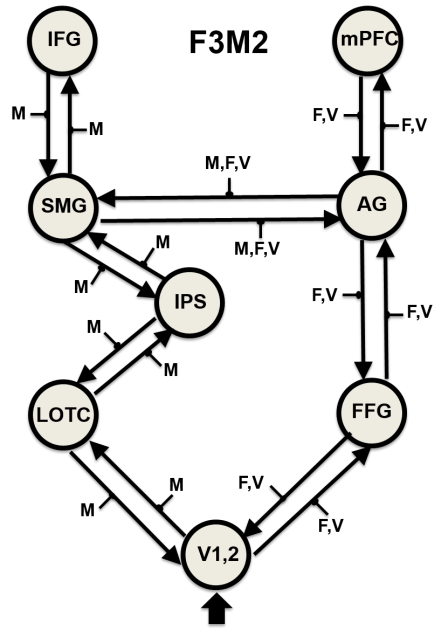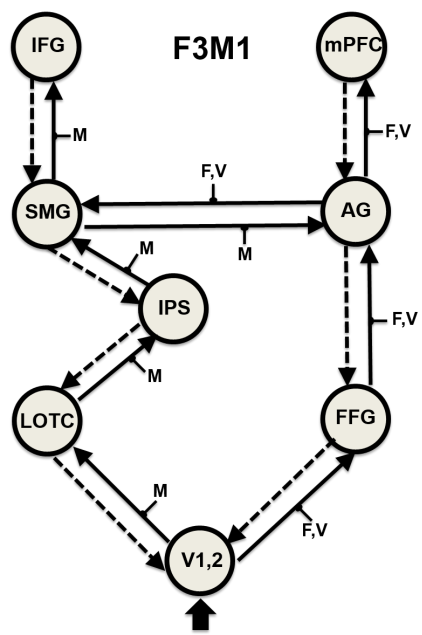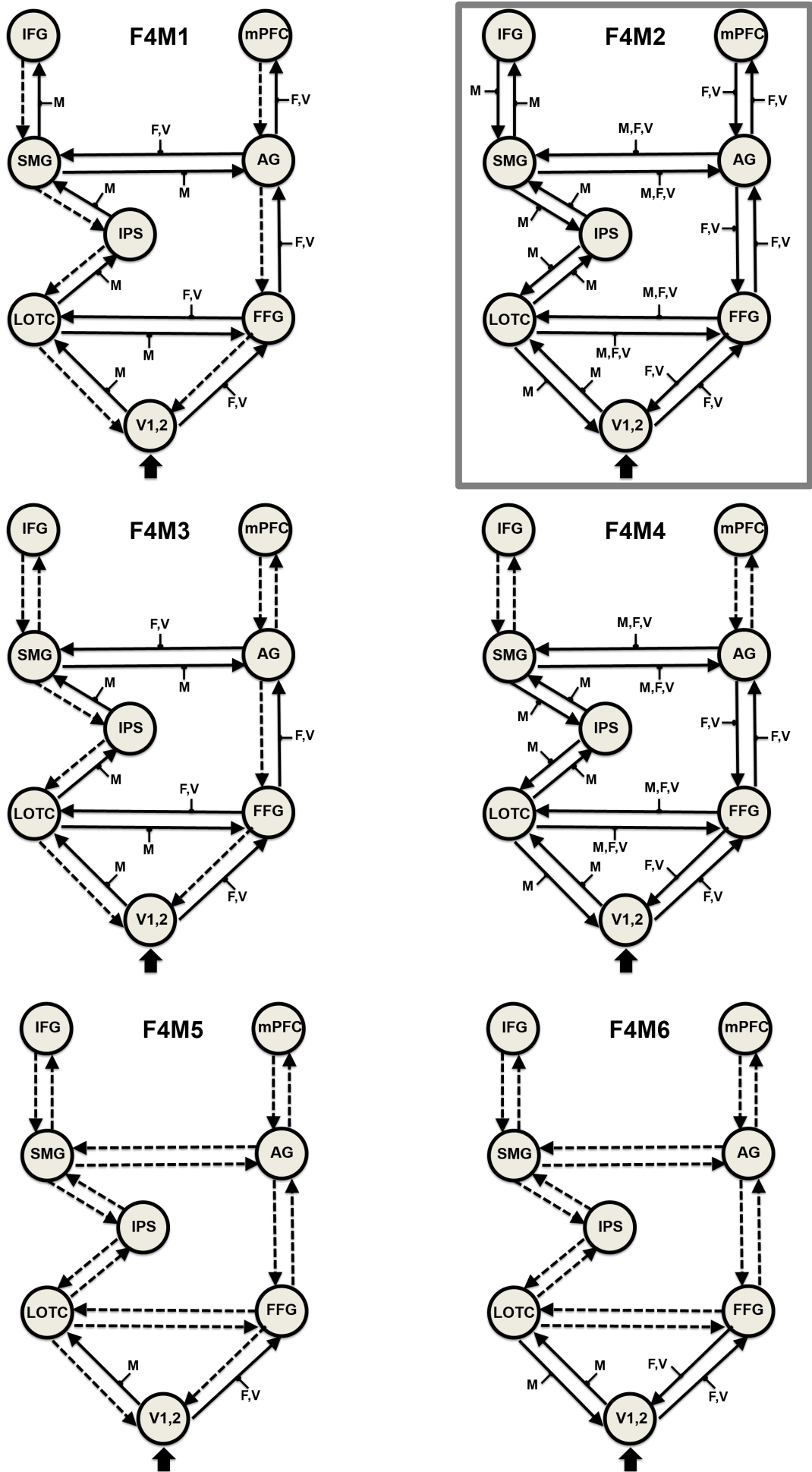
Table I. Brain regions showing significant relative increases of BOLD response associated with each comparison of interest as used for the time series extraction.

	Hemisphere	Cluster size (voxels)	max. T-value	MNI coordinates		
				x	y	z
Manipulation > (Function + Value), 2*M > (F+V)						
Middle temporal gyrus (LOTC, hOc4la)	R	1908	17.56	52	-70	-2
Middle temporal gyrus (LOTC, hOc4la)	L	1671	14.47	-58	-62	4
Intraparietal sulcus (hIP3)	L	1634	9.60	-36	-42	54
Supramarginal gyrus (PFt)	L	1634	8.22	-56	-28	40
Inferior frontal gyrus (BA 44)	L	149	8.41	-50	8	20
(Function + Value) > Manipulation, (F+V) > 2*M						
Fusiform gyrus (FG3)	R	570	9.67	34	-32	-26
			9.07	30	-50	-14
Fusiform gyrus (FG3)	L	170	8.68	-26	-48	-20
Medial prefrontal cortex (Fp2)	M	400	8.04	0	56	8
	L	400	6.49	-2	66	4
Angular gyrus (PGa)	R	242	6.17	58	-64	32
Angular gyrus (PGa)	L	155	5.26	-40	-72	48
			5.23	-50	-68	36

For each activation cluster, the coordinates in MNI space are given referring to the maximally activated voxel within an area of activation as indicated by the highest T-value. Note that in some cases sub-maxima have been used as reference coordinates for the time series extraction for DCM. All activations are significant at p<0.05 (family wise error [FWE] corrected at the voxel level) using an extent threshold of 100 voxels. The precise functional / cytoarchitectonic location of the coordinates, assessed with the anatomic toolbox (Eickhoff et al., 2005) is given in parenthesis.

LOTC, lateral occipito-temporal cortex; hOc, human occipital cortex; PFt, inferior parietal area PFt; hIP3, human intra-parietal area 3; BA, Brodmann area; FG3, fusiform gyrus area 3; Fp2, fronto-polar area 2; PGa, inferior parietal area PG anterior.

Table II. Exceedance probabilities derived from the comparison of model families (a.) and single models (b.)

a. Model families	Exceedance probability
F1	0.0201
F2	0.0178
F3	0.2263
F4	*0.7358*

b. Single models	Exceedance probability	Single models	Exceedance probability
Family 1		Family 2	
F1M1	0.0126	F2M1	0.0003
F1M2	0.0006	F2M2	0.0529
F1M3	0.0005	F2M3	0.0003
F1M4	0.0099	F2M4	0.0004
F1M5	0.0006	F2M5	0.0003
F1M6	0.0003	F2M6	0.0004
Family 3		Family 4	
F3M1	0.0003	F4M1	0.0006
F3M2	0.0997	*F4M2*	*0.5441*
F3M3	0.0003	F4M3	0.0004
F3M4	0.1219	F4M4	0.1528
F3M5	0.0000	F4M5	0.0001
F3M6	0.0003	F4M6	0.0004

Table III. DCM coupling parameters of the winning model (F4M2) in 1/s (Hz)

ROIs (left)		Intrinsics		Manipulation (M)		Function (F)		Value (V)	
Origin	Target	Mean	p (FDR)	Mean	p (FDR)	Mean	p (FDR)	Mean	p (FDR)
V1/2	FFG	0.175	0.015	–	–	0.763	<0.001	0.497	<0.001
V1/2	LOTC	0.210	0.007	1.085	<0.001	–	–	–	–
FFG	V1/2	-0.213	0.007	–	–	-0.221	n.s.	-0.072	n.s.
FFG	LOTC	-0.085	n.s.	-0.450	0.009	0.107	n.s.	-0.004	n.s.
FFG	AG	-0.031	n.s.	–	–	0.093	n.s.	0.074	n.s.
LOTC	V1/2	0.044	n.s.	-0.220	n.s.	–	–	–	–
LOTC	FFG	0.040	n.s.	0.046	n.s.	-0.358	n.s.	-0.020	n.s.
LOTC	IPS	0.257	0.004	0.501	<0.001	–	–	–	–
AG	FFG	0.028	n.s.	–	–	-0.198	n.s.	-0.128	n.s.
AG	SMG	0.024	n.s.	0.204	n.s.	-0.064	n.s.	0.067	n.s.
AG	mPFC	0.315	0.001	–	–	0.200	n.s.	-0.005	n.s.
IPS	LOTC	-0.062	n.s.	-0.370	0.018	–	–	–	–
IPS	SMG	0.063	n.s.	0.626	<0.001	–	–	–	–
SMG	AG	0.055	0.045	-0.452	0.001	0.087	n.s.	0.272	n.s.
SMG	IPS	0.043	n.s.	-0.798	0.001	–	–	–	–
SMG	IFG	0.208	0.014	0.326	<0.001	–	–	–	–
IFG	SMG	-0.117	0.045	-0.500	<0.001	–	–	–	–
mPFC	AG	-0.106	0.008	–	–	-0.194	n.s.	-0.053	n.s.

p value (FDR-corrected, False-Discovery-Rate); n.s. = not significant; – = connection not part of the tested model

V1/2, visual area 1 and 2; FFG, fusiform gyrus; LOTC, lateral occipito-temporal cortex; AG, angular gyrus; SMG, supramarginal gyrus; IPS, intraparietal sulcus; IFG, inferior frontal gyrus; mPFC, medial prefrontal cortex.

Suppl. Table SI. Brain regions showing significant relative increases of BOLD response associated with each comparison of interest.

	Hemisphere	Cluster size (voxels)	max. T-value	MNI coordinates		
				x	y	z
Manipulation > Function						
Middle temporal gyrus (LOTC, hOc4la)	R	1148	14.6	52	-70	-2
Middle temporal gyrus (LOTC, hOc4la)	L	707	10.95	-56	-64	4
Intraparietal sulcus (hIP3)	L	545	8.62	-36	-42	54
Manipulation > Value						
Middle temporal gyrus (LOTC, hOc4la)	R	2443	16.88	50	-70	-2
Middle temporal gyrus (LOTC, hOc4la)	L	2172	14.88	-58	-62	4
Supramarginal gyrus (PFt)	L	1789	10.19	-56	-32	32
Intraparietal sulcus (hIP3)	L	1789	8.86	-34	-40	44
Inferior frontal gyrus (BA 44)	L	161	8.35	-50	8	20
Superior occipital gyrus (hOc4d)	L	100	7.09	-16	-82	40
Function > Manipulation						
Fusiform gyrus (FG3)	R	1213	11.65	34	-32	-26
			10.43	30	-50	-14
Fusiform gyrus (FG3)	L	588	10.68	-26	-48	-18
Medial prefrontal cortex (Fp2)	M	173	7.42	0	56	8
Value > Manipulation						
Angular gyrus (PGa)	R	361	8.82	58	-64	32
Medial prefrontal cortex (Fp2)	M	274	7.53	-8	62	0
			7.03	0	56	8
Medial prefrontal cortex (Fp2)	M	113	6.92	-4	58	28
Function > Value						
Extra-striate cortex (hOc3d)	R	370	9.04	12	-84	26
Middle occipital gyrus (hOc4la)	L	161	8.59	-44	-80	8
Fusiform gyrus (FG3)	L	138	7.97	-36	-38	-18
Insula	R	222	6.92	56	10	-4
Value > Function (n.s.)						

For each activation cluster, the coordinates in MNI space are given referring to the maximally activated voxel within an area of activation as indicated by the highest T-value. All activations are significant at p<0.05 (family wise error [FWE] corrected at the voxel level) using an extent

threshold of 100 voxels. The precise functional / cytoarchitectonic location of the coordinates, assessed with the anatomic toolbox (Eickhoff et al., 2005) is given in parenthesis.

LOTC, lateral occipito-temporal cortex; hOc, human occipital cortex; PFt, inferior parietal area PF; hIP3, human intra-parietal area 3; BA, Brodmann area; FG3, fusiform gyrus area 3; Fp2, fronto-polar area 2; PGa, inferior parietal area PG anterior.

Suppl. Table II. Brain regions showing significant relative increases of BOLD response associated with the conjunction of Function > Manipulation and Value > Manipulation

	Hemisphere	Cluster size (voxels)	max. T-value	MNI coordinates		
				x	y	z
Conjunction of (Function > Manipulation) and (Value > Manipulation) (F>M ∩ V>M)						
Visual area (V1)	R	18	7.84	18	-102	10
Medial prefrontal cortex (Fp2)	M	93	7.03	0	56	8
Fusiform gyrus (FG3)	R	41	7.00	36	-24	-28
Fusiform gyrus (FG3)	R	13	6.21	32	-52	-12
- extending to area hOc4v	R	4	6.19	30	-78	-14
Angular gyrus (PGa, PGp)	R	11	6.25	56	-66	32
Angular gyrus (PGa)	L	1	5.81	-50	-68	36

For each activation cluster, the coordinates in MNI space are given referring to the maximally activated voxel within an area of activation as indicated by the highest T-value. All activations are significant at p<0.05 (family wise error [FWE] corrected at the voxel level). The precise functional / cytoarchitectonic location of the coordinates, assessed with the anatomic toolbox (Eickhoff et al., 2005) is given in parenthesis.

V1, visual area 1; Fp2, fronto-polar area 2; FG3, fusiform gyrus area 3; hOc4v, ventral human occipital cortex area 4; PGa, inferior parietal area PG anterior; PGp, inferior parietal area PG posterior.

Suppl. Table SIII. Individual coordinates used for time series extraction as well as the corresponding group maxima from the GLM analysis of the left hemisphere.

Subjects	MTG (LOTC, hOc4la)			IPS (hIP3)			SMG (PFt)			IFG (A 44)			FFG (FG3)			AG (PGa)			mPFC (Fp2)			V1/2		
	x	y	z	x	y	z	x	y	z	x	y	z	x	y	z	x	y	z	x	y	z	x	y	z
Subj 1	-58	-62	4	-32	-52	52	-60	-30	34	-54	6	20	-32	-52	-16	-58	-62	28	-4	60	6	-24	-100	-8
Subj 2	-54	-66	8	-40	-46	54	-50	-28	38	-50	8	36	-30	-48	-20	-52	-64	40	-4	62	10	-20	-102	0
Subj 3	-56	-68	-2	-36	-48	50	-46	-32	38	-52	6	24	-28	-66	-14	-52	-72	34	-4	64	4	-20	-100	-8
Subj 4	-58	-62	-4	-22	-64	42	-56	-32	32	-50	16	30	-32	-46	-10	-36	-72	48	-6	60	14	-24	-100	-8
Subj 5	-48	-76	2	-38	-44	42	-50	-30	42	-50	6	30	-34	-50	-20	-54	-62	36	-2	58	8	-16	-98	-12
Subj 6	-50	-70	0	-40	-50	60	-62	-28	40	-52	8	20	-34	-48	-22	-54	-62	40	-2	54	10	-18	-100	-14
Subj 7	-54	-68	0	-36	-54	54	-48	-28	40	-60	14	26	-40	-46	-16	-56	-66	34	-6	58	16	-24	-102	-14
Subj 8	-50	-62	8	-38	-38	42	-54	-26	28	-52	8	20	-24	-66	-16	-50	-56	36	-8	66	-2	-28	-100	-8
Subj 9	-54	-74	0	-24	-60	48	-64	-30	38	-48	4	24	-40	-62	-20	-48	-70	26	-6	58	4	-26	-100	-10
Subj 10	-62	-62	2	-36	-48	56	-62	-22	38	-56	10	28	-32	-48	-18	-36	-72	44	-6	68	2	-16	-98	-14
Subj 11	-52	-66	-2	-40	-48	54	-52	-26	34	-50	6	18	-30	-52	-20	-44	-60	42	-8	68	4	-10	-98	-10
Subj 12	-46	-70	10	-30	-60	54	-62	-26	44	-56	8	24	-30	-56	-18	-42	-70	28	-2	54	6	-28	-100	-8
Subj 13	-54	-68	-8	-38	-44	46	-56	-26	40	-60	8	14	-32	-50	-14	-40	-66	36	-2	58	16	-20	-100	-8
Subj 14	-52	-72	-8	-40	-50	60	-54	-30	34	-52	12	36	-28	-46	-12	-46	-68	34	-6	54	4	-14	-100	-2
Subj 15	-58	-58	12	-36	-48	56	-48	-28	38	-54	8	16	-32	-54	-18	-52	-60	40	-4	52	6	-10	-100	-10
Subj 16	-52	-62	6	-38	-44	50	-50	-28	42	-50	4	28	-36	-46	-24	-50	-66	42	-4	62	18	-18	-100	-2
Subj 17	-52	-70	8	-30	-56	54	-42	-36	40	-54	12	28	-28	-58	-18	-34	-70	46	-2	60	20	-18	-100	-8
Mean	**-54**	**-67**	**2**	**-35**	**-50**	**51**	**-54**	**-29**	**38**	**-53**	**8**	**25**	**-32**	**-53**	**-17**	**-47**	**-66**	**37**	**-4**	**60**	**9**	**-20**	**-100**	**-8**
Group Max	-58	-62	4	-36	-42	54	-56	-28	40	-50	8	20	-26	-48	-20	-50	-68	36	0	56	8	-16	-98	-10

The functional/ cytoarchitectonic area, in which the majority of the presented individual MNI coordinates clustered are given in parenthesis. For details on the corresponding group maxima of the GLM analysis and the respective contrast applied, please see Table I. The coordinates for the visual cortex (common input region) were detected by a conjunction analysis of the three experimental conditions versus baseline (M versus baseline, F versus baseline, V versus baseline).

MTG, middle temporal gyrus; LOTC, lateral occipito-temporal cortex; IPS, intraparietal sulcus; SMG, supramarginal gyrus; IFG, inferior frontal gyrus; FFG, fusiform gyrus; AG, angular gyrus; mPFC, medial prefrontal cortex; V1/2, visual area 1 and 2.

Suppl. Table SIV

List of the 40 target tools (in alphabetical order) together with the (recipient) objects used in Function knowledge (F) task and the respective coins and banknotes in the Value knowledge (V) task.

Items	Function knowledge task (F)		Value knowledge task (V)	
bottle opener	beer bottle	wine bottle	5 € banknote	20 € banknote
bread knife	bread	piece of wood	10 € banknote	50 € banknote
cake server	bread	cake	10 € banknote	50 € banknote
carpet beater	Shirt	carpet	10 € banknote	50 € banknote
computer mouse	television	computer	1 € coin	10 € banknote
corkscrew	beer bottle	wine bottle	5 € banknote	20 € banknote
dart	target disk	golf ball	1 € coin	10 € banknote
drumstick	drum	violin	50 € banknote	10 € banknote
eraser	pen	pencil	5 € banknote	1 € coin
garden pruner	rose	piece of wood	10 € banknote	50 € banknote
hammer	screw	nail	10 € banknote	50 € banknote
hand broom	dustpan	squeegee	20 € banknote	2 € coin
hand mixer	pan	baking bowl	20 € banknote	2 € coin
ice cream scooper	ice cream in a cone	iced-lolly	50 € banknote	10 € banknote
ice scraper	motorbike	car	5 € banknote	20 € banknote
light switch	ceiling light	torch (flashlight)	50 € banknote	10 € banknote
lighter	ladyfinger (biscuit)	cigarette	2 € coin	10 € banknote
match	light bulb	candle	5 € banknote	1 € coin
needle	thread	shoestring	5 € banknote	1 € coin
paint roller	paint can	watercolors	50 € banknote	10 € banknote
paper clip	tape	papers	5 € banknote	1 € coin
pizza knife	cake	pizza	50 € banknote	5 € banknote
plug	plug socket	light switch	20 € banknote	2 € coin
remote control	washing machine	television	10 € banknote	1 € coin
salt shaker	egg	cake	20 € banknote	5 € banknote
saw	bread	piece of wood	1 € coin	20 € banknote
scissors	tape	eraser	5 € banknote	50 € banknote
screwdriver	screw	nail	50 € banknote	5 € banknote
shoe brush	leather shoe	rubber boot	5 € banknote	20 € banknote
shoe horn	sandal	shoe	50 € banknote	5 € banknote
spatula	pan	pot	5 € banknote	50 € banknote
sponge	blackboard	notebook	1 € coin	10 € banknote

spoon	ashtray	soup bowl	5 € banknote	50 € banknote
stapler	pencil	papers	20 € banknote	10 € banknote
teapot	tea cup	egg cup	1 € coin	10 € banknote
tennis racket	tennis ball	shuttlecock	50 € banknote	20 € banknote
violin bow	guitar	violin	50 € banknote	5 € banknote
water bottle	egg cup	glass	10 € banknote	1 € coin
watering can	vase of flowers	potted flower	50 € banknote	10 € banknote
wooden spoon	pot	boiler	2 € coin	10 € banknote